



## Impact of land use on the hydraulic properties of the topsoil in a small French catchment

E. Gonzalez Sosa, I. Braud, J. Dehotin, L. Lassabatère, R. Angulo Jaramillo, M. Lagouy, F. Branger, C. Jacqueminet, S. Kermadi, K. Michell

### ► To cite this version:

E. Gonzalez Sosa, I. Braud, J. Dehotin, L. Lassabatère, R. Angulo Jaramillo, et al.. Impact of land use on the hydraulic properties of the topsoil in a small French catchment. *Hydrological Processes*, Wiley, 2010, 24 (17), p. 2382 - p. 2399. <10.1002/hyp.7640>. <hal-00507313>

**HAL Id: hal-00507313**

**<https://hal.archives-ouvertes.fr/hal-00507313>**

Submitted on 30 Jul 2010

**HAL** is a multi-disciplinary open access archive for the deposit and dissemination of scientific research documents, whether they are published or not. The documents may come from teaching and research institutions in France or abroad, or from public or private research centers.

L'archive ouverte pluridisciplinaire **HAL**, est destinée au dépôt et à la diffusion de documents scientifiques de niveau recherche, publiés ou non, émanant des établissements d'enseignement et de recherche français ou étrangers, des laboratoires publics ou privés.

1

1 **Impact of land use on the hydraulic properties of the topsoil**

2 **in a small French catchment**

3

4 E. Gonzalez-Sosa,<sup>1,2</sup> I. Braud,<sup>1\*</sup> J. Dehotin,<sup>1</sup> L. Lassabatère,<sup>3</sup> R. Angulo-Jaramillo,<sup>4,5</sup>

5 M. Lagouy<sup>1</sup>, F. Branger<sup>1</sup>, C. Jacqueminet<sup>6</sup>, S. Kermadi<sup>6</sup>, K. Michell<sup>6</sup>

7<sup>1</sup> Cemagref, UR HHLY, CP 220, 3bis Quai Chauveau, 69336 Lyon Cédex 9, France

8<sup>2</sup> DEFI-CIAQ, Université de Querétaro, CU Cerro de las Campanas. S/N. Centro. 6900  
9Queretaro, Qro., Mexico

10<sup>3</sup> Laboratoire Central des Ponts et Chaussées, Division Eau et Environnement, Route de  
11Bouaye, 44381 Bouguenais Cedex, France.

12<sup>4</sup>Université de Lyon, ENTPE, rue Maurice Audin, 69518 Vaulx-en-Velin, France

13<sup>5</sup> LTHE, CNRS, BP 53, 38041 Grenoble Cedex 9, France

14<sup>6</sup>Université de Lyon, UMR CNRS EVS, 18 rue de Chevreur, F-69 364 Lyon Cedex, France

15

16

17

18

19

20\* Correspondance to: Isabelle Braud, Cemagref, UR HHLY, CP 220, 3bis Quai Chauveau,  
2169336 Lyon cedex 9, France

22E-mail : [Isabelle.Braud@cemagref.fr](mailto:Isabelle.Braud@cemagref.fr)

23

24

25

26*Hydrological Processes*, 2010, Vol 24, 2382-2399, DOI: 10.1002/hyp.7640

1

## 1 Abstract

2 The hydraulic properties of the topsoil control the partition of rainfall into infiltration and  
3 runoff at the soil surface. They must be characterized for distributed hydrological modelling.  
4 This study presents the results of a field campaign documenting topsoil hydraulic properties  
5 in a small French suburban catchment (7 km<sup>2</sup>) located near Lyon, France. Two types of  
6 infiltration tests were performed: single ring infiltration tests under positive head and tension  
7 disk infiltration using a mini-disk. Both categories were processed using the BEST –*Beerkan*  
8 Estimation of Soil Transfer parameters- method to derive parameters describing the retention  
9 and hydraulic conductivity curves. Dry bulk density and particle size data were also sampled.  
10 Almost all the topsoils were found to belong to the sandy loam soil class. No significant  
11 differences in hydraulic properties were found in terms of pedologic units, but the results  
12 showed a high impact of land use on these properties. The lowest dry bulk density values  
13 were obtained in forested soils with the highest organic matter content. Permanent pasture  
14 soils showed intermediate values, whereas the highest values were encountered in cultivated  
15 lands. For saturated hydraulic conductivity, the highest values were found in broad leaved  
16 forests and small woods. The complementary use of tension disk and positive head infiltration  
17 tests highlighted a sharp increase of hydraulic conductivity between near saturation and  
18 saturated conditions, attributed to macroporosity effect. The ratio of median saturated  
19 hydraulic conductivity to median hydraulic conductivity at a pressure of -20 mm of water,  
20 was about 50. The study suggests that soil texture, such as used in most pedo-transfer  
21 functions, might not be sufficient to properly map the variability of soil hydraulic properties.  
22 Land use information should be considered in the parameterizations of topsoil within  
23 hydrological models to better represent *in situ* conditions, as illustrated in the paper.

24

1

1Keywords: soil hydraulic properties, infiltration tests, BEST method, land use impact,  
2hydraulic properties mapping

1

## 1 INTRODUCTION AND CONTEXT

2

3 Soil surface thermal and hydraulic properties control heat and water exchange at the soil  
4 vegetation atmosphere interface through their impact on infiltration and the surface energy  
5 balance. Therefore, they play a central role in the correct understanding and modelling of  
6 water balance, surface processes, evapotranspiration, groundwater recharge, erosion or  
7 pollutant transport. Human activities such as agricultural practices (ploughing, sowing),  
8 changes in land use related to urbanisation, industrial activity, deforestation or reforestation of  
9 abandoned agricultural land can significantly affect topsoil and first layers hydraulic  
10 properties. The accurate representation of soil hydraulic properties within hydrological  
11 models is therefore necessary to reliably represent the water balance and hydrological  
12 responses. In many hydrological models, soil hydraulic properties are determined based on  
13 pedo-transfer functions. These functions relate easily accessible soil properties such as soil  
14 texture (e.g. Clapp and Hornberger, 1978; Cosby *et al.*, 1984) or soil texture, organic matter  
15 content and dry bulk density (e.g. Rawls and Brackensiek, 1985; Verecken *et al.*, 1989;  
16 Wösten, 1997) to soil hydraulic properties (retention and hydraulic conductivity curves).  
17 Existing pedo-transfer functions have been in general calibrated on limited soil samples and  
18 are often region specific. As an illustration, the pedotransfer functions of Cosby *et al.*, (1984)  
19 and Rawls and Brackensiek (1985) were calibrated on US soils. Verecken *et al.* (1989) used  
20 soil samples from Belgium, and Wösten (1997) the HYPRES European soil data base  
21 (Wösten *et al.*, 1999). Different conclusions have been reached about the use of pedotransfer  
22 functions in hydrological models. Some studies have concluded that existing pedo-transfer  
23 functions are adequate (e.g. Islam *et al.*, 2006) whereas other authors question their usefulness  
24 for a correct assessment of hydrological water balances (e.g. Sobieraj *et al.*, 2001; Gutman  
25 and Small, 2005). Wösten *et al.* (2001) underline the usefulness of pedotransfer functions but

2

4

1discourage their use for soils that are outside their range of applications, while calling for the  
2collection of large data sets to document soil hydraulic properties worldwide.

3The present study is based on these recommendations and contributes to the documentation of  
4soil hydraulic properties in a small French suburban catchment. Suburban catchments  
5generally experience a large and quick land-use change, such as an increase of impervious  
6areas, but also sometimes, desertion of farming lands that turn into fallow lands, and finally  
7into sporadic deciduous forests. Rivers and runoff are also affected through straightening of  
8natural water courses and runoff concentration into pipes for instance. A higher proportion of  
9built infrastructures has a significant impact on hydrologic and ecosystem functions and often  
10result in excess runoff, lower groundwater recharge and pollution (e.g., Bras and Perkins,  
111975; Desbordes, 1989; Chocat *et al.*, 2001; Booth *et al.*, 2002; Randhir, 2003; Matteo *et al.*,  
122006; Marsalek *et al.*, 2007). The vulnerability of these areas to floods, droughts and water  
13quality problems is therefore increased.

14The Yzeron catchment (150 km<sup>2</sup>) is located to the south-west of Lyon city (Figure 1). This  
15catchment is representative of many suburban catchments. Since the fifties, it has experienced  
16rapid changes of land use, due to the vicinity of Lyon city. Two different trends can be  
17observed since the middle of the 20<sup>th</sup> century. The first one is an increase of the catchment  
18urbanisation, with a full urbanised area in the downstream part. The second trend is a decrease  
19of cultivated land explained by the urbanisation, but also by an increase of the forested areas  
20in relation with the decline of agricultural activities (Gnouma, 2006). In recent years, several  
21problems have been identified: an increase in the frequency of flooding (Radojevic, 2002),  
22increased pollution problems (Lafont *et al.*, 2006), and increased erosion of the river banks  
23associated with adverse effects on water quality (Schmitt *et al.*, 2008). The water responsible  
24for these flooding events comes mainly from the rural part of the catchment, but its effect can  
25be enhanced by fast contributions from urbanised zones having short runoff lag time

1

1(Radojevic, 2002). These disorders must be reduced to comply with the requirements of the  
2water framework directive. It is therefore important to better quantify the impact of land use  
3changes on the hydrological regime of this catchment. For this purpose, a distributed  
4hydrological model of the catchment is being developed, that takes into account both the rural  
5and the urbanised areas. Given the importance of rural areas on the Yzeron regime, it was  
6necessary to acquire improved knowledge on the soil hydraulic properties within the  
7catchment and propose rules for their specification in the elementary meshes of the distributed  
8hydrological model (from a few hectares to a few km<sup>2</sup>). This task is of course challenging,  
9because it is not possible to measure soil hydraulic properties everywhere and we wanted to  
10propose alternative solutions to the use of pedo-transfer functions only, by introducing *in situ*  
11observations in the mapping process.

12The objectives of the study were the following: (i) to document the spatial variability of soil  
13hydraulic properties (including both the retention and hydraulic conductivity curves) within  
14the catchment using relevant *in situ* measurements and an adequate sampling strategy; (ii) to  
15analyse the links between the spatial variability of hydraulic properties and pedology and land  
16use; (iii) to use these measurements to derive rules for the mapping of soil hydraulic  
17properties as required in distributed hydrological modelling.

18

## 19MATERIALS AND METHODS

### 20*Catchment description*

21The Yzeron catchment is located south-west of Lyon city in the “Mont du Lyonnais” area  
22(Figure 1). The topography ranges from a maximum of 917 m above sea level in the western  
23part to a minimum of 162 m at the outlet. The highest slopes are encountered in the western  
24part of the catchment and along the river network and the lowest slopes are located in the

1

1eastern part (Figure 1). The geology is composed mainly of gneiss and granite. The average  
2annual rainfall is 800 mm and the average annual minimum and maximum temperatures are  
36.8 °C and 15.8 °C, respectively (Gnouma, 2006). The catchment forms part of a long term  
4observatory called Observatoire de Terrain en Hydrologie Urbaine (OTHU, 2010), dedicated  
5to the study of the impact of urbanisation on hydrology. In this framework, two sub-  
6catchments have been monitored since 1997. The first one, the Mercier catchment (7 km<sup>2</sup>) is  
7considered as a natural catchment and is covered mainly with forests and crops. The second  
8one, the Chaudanne catchment (2.5 km<sup>2</sup>) is mainly covered with crops and urbanised areas  
9(Figure 1). The Mercier catchment shows a large spatial variability of soils, with the presence  
10of 8 soil pedological units over a total of 22 present within the whole Yzeron catchment,  
11according to the Sol Info Rhône Alpes pedology map (SIRA, 2010). The Mercier catchment  
12soils are also representative of the rural area of the Chaudanne catchment. The study  
13presented here is therefore focused on the Mercier catchment. In this basin, the elevation  
14ranges from 400 m and 800 m with a marked topography and slopes commonly higher than  
1510%. The land use is dominated by forest, pasture and crops, although a significant part of the  
16catchment is affected by human activity with the existence of small villages and a quite dense  
17road network.

18

### 19*Sampling strategy*

20The sites were selected to include the maximum combinations of factors that can influence  
21soil hydraulic properties such as pedology and land use. For this purpose, we used the  
22pedology map, provided by Sol Info Rhône Alpes at scale 1/250000 (Figure 2, SIRA, 2010)  
23and the 2000 Corine Land Cover map provided by the Service de l'Observation et des  
24Statistiques (SOeS, 2010). The distribution from the land use map showed that the forest area  
25(mountain) represents about 33%, pasture 32% and complex cultivation pattern accounts for



1

about 30% of the total basin area. Urbanised surface is less than 6% of the total surface. Regarding soil classes, soil 102 (loamy sand and clayey sand – see Table I) covers more than 35% of the basin area. From this analysis, nine soil classes and six land uses from the Corine map were retained that accounted for most of the total area and a first selection of sites was performed in order to sample the maximum of land use/pedology combinations (17 over a total of 38 covering 90% of the catchment surface). Sites accessibility was also taken into account in the final selection. A field survey refined the selection and the land use description, especially for crops where the Corine land cover map was not detailed. Finally 20 locations were retained and sampled (Figure 2). Their distribution in terms of pedology (Soil Cartographic Units –SCU-) and land use, as retrieved from the field, is shown in Table I. The measured points within the sites were located at least 10 m from the fields edges. With regard to topography, most of the sites were located on slopes, very few in flat zones. At the 320 locations, samples were collected in order to characterize the soil texture and the dry bulk density. Infiltration tests using single ring and mini-disk infiltrometers were performed. The field survey was restricted to the topsoil layer. The location of each infiltration test was measured using a GPS (3 m in  $x$  and  $y$ ). The experimental protocols are described below.

17

### 18 *Soil texture and dry bulk density measurements*

19 Twenty-eight topsoil samples of 250-300 g were collected using augers and were analysed to 20 derive the soil particle size distribution function. Five classes were considered (clay, fine silt, 21 coarse silt, fine sand, coarse sand) corresponding to the following fractions (<2, 2-20, 20-50, 22 250-200, 200-2000  $\mu\text{m}$ ) and were determined according to the French standard (NF X 31-107 23 norm), which involves sieving for the fractions >50  $\mu\text{m}$  and sedimentation below 50  $\mu\text{m}$ . 24 Organic matter content was also determined using the NF ISO 10694 standard. All the 25 analyses were done at the INRA soil laboratory in Arras .

2

8

1

1To characterize the topsoil *A* horizon, the dry bulk density was measured using samples  
2collected in the 0-2.5 cm depth and 0-5 cm depth layers. These samples were collected  
3following the ISO NF X31-501 standard. The dry bulk density,  $\rho_d$ , allows the derivation of  
4porosity once assumed a certain value for the particle density,  $\rho_s$ . In this study we used the  
5commonly used value of  $\rho_s = 2650 \text{ kg m}^{-3}$  and the porosity,  $\varepsilon$ , was calculated as:

$$6 \quad \varepsilon = 1 - \frac{\rho_d}{\rho_s} \quad (1)$$

### 7Infiltration tests

8The field campaign was conducted from October 6 to October 10 2008 by a team of five  
9persons. At each of the twenty selected locations, infiltration tests were performed using two  
10techniques: Mini Disk Infiltrometer (MDI) (in general two replicates per location) and single  
11ring (SR) or *Beerkan* method (Braud *et al.*, 2005) (three replicates per location). Their  
12distribution with respect to pedological cartographic units and land uses is shown in Table I.  
13Braud *et al.* (2005) proposed an experimental protocol for the single ring infiltration tests,  
14with cylinders of 5-15 cm in diameter. According to this protocol, about 8-15 equal volumes  
15of water must be poured successively into the cylinders. The infiltration times of these water  
16volumes are measured. In our study, the cylinders used for the SR tests were 400 mm in  
17diameter and 225 mm in height. They were much larger than recommended by Braud *et al.*  
18(2005). The reason of this choice is the wish to average the soil spatial heterogeneity by  
19sampling a larger surface, in order to obtain measures representative of the fields. As a  
20consequence, the infiltration protocol had to be modified as compared to Braud *et al.* (2005).  
21Before each SR test, the litter and vegetation leaves were removed, as in Bodhinayake and Si  
22(2004). If necessary, the vegetation was cut but roots were left in place. The cylinders were  
23inserted 2-5 cm deep into the soil, in order to ensure water tightness and avoid leaks, without  
24perturbing too much the 3-D water flow. In all cases 12 L of fresh (15-18 °C) water were

1

1 poured within a plastic sheet, sealed to the cylinder, to minimize the disturbances in topsoil  
2 that frequently occur when water is added directly. The plastic sheet was then removed and  
3 the chronometer was started. The initial height was measured using a ruler. Then the  
4 infiltration height as a function of elapsed time was followed by reading the ruler. During the  
5 first minutes, small time intervals of a few seconds were used and the time interval was  
6 increased after 3 or 5 minutes (Herman *et al.* 2003). The operation was terminated when all  
7 the water had infiltrated the soil. Two soil samples were also collected for measurement of  
8 the initial and final gravimetric water contents (g water per g solids). For the final water  
9 content sampling, small cylinders of 43 mm in diameter and 28 mm in height were used.  
10 These samples enable us to obtain additional measurements of the dry bulk density.

11 For the MDI infiltration tests, we used the tension Mini-disk Infiltrometer of 135 ml in  
12 volume water capacity and 22.5 mm in radius (Decagon Devices Inc., Pullman, WA). The  
13 detritus and dead leaves were also removed before the tests started. A small layer of soil  
14 (Horizon O < 5 cm) of less than 2 cm was also removed. It was required in order to carry out  
15 the tests on horizontal surfaces and ensure the stability of the apparatus and a good contact  
16 between the infiltrometer membrane and the soil. For this we used a thin layer (< 1mm) of  
17 fine sand. The surface pressure was set to -20 mm for all the MDI infiltration tests.

18

### 19 *Derivation of retention and hydraulic conductivity curves parameters using the BEST method*

20 The infiltration tests were used to determine the retention curve  $h(\theta)$ , relating the soil water  
21 pressure  $h$  (m) to the soil volumetric water content  $\theta$  ( $\text{m}^3 \text{m}^{-3}$ ) and the hydraulic conductivity  
22 curve  $K(\theta)$  relating the soil hydraulic conductivity  $K$  ( $\text{m s}^{-1}$ ) to the soil water content. The  
23 retention curve was modeled using the van Genuchten (1980) approach:

1

$$1 \quad \frac{\theta}{\theta_s} = \left\{ 1 + \left( \frac{h}{h_{VG}} \right)^n \right\}^{-m} \quad (2)$$

$$2 \text{with} \quad n = \frac{k}{1 - m} \quad (3)$$

3where  $\theta_s$  is the saturated water content ( $\text{m}^3 \text{m}^{-3}$ ),  $h_{VG}$  (m) is a normalization parameter for the  
 4water pressure,  $m$  and  $n$  are shape parameters (-) and  $k$  is an integer which can be chosen to be  
 51 (Mualem, 1976) or 2 (Burdine, 1953). A value of  $k=2$  was used in the following. A value  
 6of  $k=1$  could have been used either as Haverkamp *et al.* (2005) provide relationships between  
 7the various formulations. Eq. (2) assumes that the residual water content at large pressure is  
 8zero.

9The hydraulic conductivity curve was modeled using the Brooks and Corey (1964) model:

$$10 \quad K(\theta) = K_s \left( \frac{\theta}{\theta_s} \right)^\eta \quad (4)$$

11where  $K_s$  ( $\text{m s}^{-1}$ ) is the saturated hydraulic conductivity and  $\eta$  is a shape parameter (-) related  
 12to  $m$  and  $n$  by:

$$13 \quad \eta = \frac{2}{mn} + 2 + p \quad (5)$$

14where  $p$  is a tortuosity parameter equal to 0 (Childs and Collis-George, 1950), 0.5 (Mualem,  
 151976) or 1 for the Burdine (1953) model. A value of 1 was used in this study to be consistent  
 16with the choice of the Burdine (1953) model for the retention curve in Eq. (3).

17At each location, the values of the parameters of the retention and hydraulic conductivity  
 18curves as described by Eqs. (2) and (4), namely the shape parameters  $m$ ,  $n$  and  $\eta$  and the  
 19structure parameters  $\theta_s$ ,  $h_{VG}$  and  $K_s$  were calculated. It was done using the BEST (*Beerkan*  
 20*Estimation of Soil Transfer parameters*) method proposed by Lassabatère *et al.* (2006). The  
 21first step of the BEST method corresponds to the estimation of the shape parameters  $m$ ,  $n$  and

1

1  $\eta$  from the soil particle size distribution data. Details can be found in Lassabatère *et al.* (2006)  
 2 and are not reported here.

3 The second step is the optimisation of the infiltration tests in order to derive the structural  
 4 parameters  $\theta_s$ ,  $h_{VG}$  and  $K_s$ . In this study, the saturated water content,  $\theta_s$ , was determined from  
 5 field final water content and dry bulk density and therefore only  $h_{VG}$  and  $K_s$  were derived from  
 6 the optimisation of the infiltration tests. Two equations were used for this purpose.

7 For short to medium time steps, the BEST method uses an analytical approximation of the full  
 8 3D infiltration,  $I_{3D}(t)$  (m), equation proposed by Haverkamp *et al.* (1994) for the interpretation  
 9 of infiltration tests:

$$10 \quad I_{3D}(t) = S\sqrt{t} + \left[ \frac{\phi S^2}{R(\theta_0 - \theta_i)} + K_i + \frac{2 - \beta}{3}(K_0 - K_i) \right] t \quad (6)$$

11 where  $S$  is the sorptivity ( $\text{m s}^{-1/2}$ );  $R$  is the radius of the infiltrometer (m),  $\theta_i$  is the initial  
 12 water content and  $\theta_0$  is the final water content,  $K_i$  is the initial hydraulic conductivity ( $\text{m s}^{-1}$ )  
 13 and  $K_0$  ( $\text{m s}^{-1}$ ) is the final one.  $K_0 = K(h_0)$ , where  $h_0$  (m) is the water pressure at the soil  
 14 surface (positive for single ring infiltration tests and negative for mini-disk infiltration tests).  
 15 For the parameters  $\beta$  and  $\phi$ , we used the value of  $\phi=0.75$  and  $\beta=0.6$ , shown to apply for most  
 16 soils when  $\theta_i < 0.25 \theta_s$  (Smettem *et al.*, 1994; Haverkamp *et al.*, 1994). The sorptivity  
 17  $S(\theta_i, \theta_0)$  is a function of initial and final water content but notation  $S = S(\theta_i, \theta_0)$  will be used  
 18 for the sake of simplicity.

19 The approximation provided by Eq.(6) is valid only for times  $t_i$  lower than a maximum value  
 20 given in Lassabatère *et al.* (2006):

$$21 \quad t_{\max} = \frac{1}{4(1 - B)^2} t_{\text{grav}} \quad (7)$$

$$22 \text{ where } B = \frac{K_i}{K_0} + \frac{2 - \beta}{3} \left( 1 - \frac{K_i}{K_0} \right) = \left( \frac{\theta_i}{\theta_0} \right)^\eta + \frac{2 - \beta}{3} \left( 1 - \left( \frac{\theta_i}{\theta_0} \right)^\eta \right) \quad (8)$$

1

1and 
$$t_{grav} = \left( \frac{S}{K_0} \right)^2 \quad (9)$$

2 $t_{grav}$  is the gravity time which corresponds to the time at which gravity begins to dominate the  
 3flow process (Philip, 1969).

4For long time steps, Haverkamp *et al.* (1994) showed that the asymptotic infiltration can be  
 5written (subscript <sub>3D</sub> is omitted in the following for simplicity):

6 
$$I_{\infty} = \left[ K_0 + \frac{\phi S^2}{R(\theta_0 - \theta_i)} \right] t + \frac{S^2}{2(K_0 - K_i)(1 - \beta)} \ln \left( \frac{1}{\beta} \right) \quad (10)$$

7which corresponds to a linear variation with time. For long time steps, the infiltration flux is a  
 8constant given by the slope of the curve  $I(t)$  as defined by Eq. (10):

9 
$$q_{\infty} = K_0 + \frac{\phi S^2}{R(\theta_0 - \theta_i)} = K_0 + AS^2 \quad (11)$$

10with 
$$A = \frac{\phi}{R(\theta_0 - \theta_i)} \quad (12)$$

11Data for large time steps are used to fit Eq. (10) using a simple regression analysis and derive  
 12the  $q_{\infty}$  estimate. For short times steps, we used the method proposed by Lassabatère *et al.*  
 13(2006) to optimize the sorptivity. The reader can refer to this paper for more details.

14Note that, up to this step, the method can be applied both for infiltration test under suction or  
 15with a positive pressure head. Therefore it can be used for the interpretation of both the mini-  
 16disk and single ring infiltration tests.

17On the other hand, the estimation of the normalization parameter  $h_{VG}$  can only be performed  
 18from the SR infiltration (Braud *et al.*, 2005) using:

19 
$$h_{VG} = - \frac{S^2}{c_{p-VG}(\theta_s - \theta_i)K_s \left[ 1 - \left( \frac{\theta_i}{\theta_s} \right)^{\eta} \right]} \quad (13)$$

1

1 where  $c_{p\_VG}$  is a texture dependent factor, the expression of which is given by Haverkamp *et al.* (1998):

$$3 \quad c_{p\_VG} = \Gamma\left(1 + \frac{1}{n}\right) \left\{ \frac{\Gamma\left(m\eta - \frac{1}{n}\right)}{\Gamma(m\eta)} + \frac{\Gamma\left(m\eta + m - \frac{1}{n}\right)}{\Gamma(m\eta + m)} \right\} \quad (14)$$

4 where  $\Gamma$  is the classical incomplete Gamma function.

5 Up to now, only positive head infiltration tests have been analysed using the BEST method  
6 (de Souza *et al.*, 2008; Mubarak *et al.*, 2009; Xu *et al.*, 2009). The only exception is the case  
7 study by Scalenghe and Ferraris (2009) that also analysed tension-disk infiltration tests with  
8 the method. To our knowledge, it is also the first time that the method is used on terrain with  
9 a significant slope and using cylinders with so large diameters.

10

### 11 *Statistical analysis of data*

12 The data were analysed using statistical tests from the R packages (R Development Core  
13 Team, 2004). Kolmogorov-Smirnov or  $\chi^2$  tests were performed to test the hypothesis of  
14 normal distribution of the data. When appropriate, i.e. independent normal distribution for  
15 residuals, along with equality in variances, Student t-tests were performed to study the degree  
16 of significance of differences in averages amongst different factors (pedology and land use  
17 classes). Otherwise, non parametrical tests (Kruskal-Wallis / Wilcoxon tests) were performed.  
18 Results are presented in terms of the critical probability  $p$  that quantifies the risk to be wrong  
19 when rejecting the null hypothesis (no effect and no difference). If  $p < 0.05$  (respectively  
20  $< 0.10$ ), then the hypotheses of equality of mean/variance/distribution is rejected at the 5%  
21 (respectively 10%) level and the difference amongst classes can be considered as significant  
22 at this level.

2

14

1

1The replicates were considered as independent samples in the statistical analysis. Except three  
2points, the sampled points within the same field were distant from more than 20 m. The  
3distance between fields was more than 50-100 m. In the recent synthesis proposed by van der  
4Keur and Iversen (2009), soil porosity is reported to have a spatial correlation ranging from 0  
5to about 75 m from three different studies. Saturated hydraulic conductivity spatial correlation  
6is reported to range between 0 and about 40 m in six studies. These figures and the fact that  
7most of the points were collected in different fields, even at the same site, justify our  
8independence hypothesis of the measurement points.

## 9RESULTS

10In this section, we discuss the results in terms of soil texture, soil porosity, fitting of the  
11infiltration tests. Then, results of the single ring infiltration tests, and of mini-disk infiltration  
12tests, are discussed. Finally, results are summarised in terms of retention and hydraulic  
13conductivity curves. A mapping of the topsoil surface properties over the Mercier catchment  
14is also proposed.

### 15Soil texture

16The soil particle size distribution was measured using 28 samples of the topsoil. Figure 3a  
17presents the results for clay, fine and coarse silt, fine and coarse sand. Table II summarizes  
18these results as well as those of the shape parameters  $n$  and  $\eta$  of the retention and hydraulic  
19conductivity curves. Figure 4 presents all the sample points in the USDA textural triangle. It  
20shows that all the topsoil A horizons belong to the sandy loam soil class except one loam, one  
21silty clay loam and two loamy sands. However, the variability of texture within the sandy  
22loam class is quite large. The soils have generally a coarse texture, with an average sand  
23content of 67.5%. The coefficient of variation of the sand fractions is about 20%. The clay  
24content is 13% on average, with a lower coefficient of variation (14%). The silt content is



1

1 about 20% on average, with the largest coefficient of variation (30%). The  $\chi^2$  goodness of fit  
2 test showed that the Gaussian distribution was acceptable for all the fractions ( $p > 0.10$ ). The  
3 Kruskal-Wallis test showed no significant differences in distribution in terms of Soil  
4 Cartographic Unit (SCU) for all the fractions except the fine sand fraction at the 5% level  
5 ( $p = 0.02$ ), the coarse silt fraction ( $p = 0.09$ ), and the coarse sand fraction ( $p = 0.094$ ) at the 10%  
6 level.

7 The organic matter content shows a high variability with a coefficient of variation of about  
8 50% ranging from 2 to 13%, with the highest content in forest soils and pasture. The Gaussian  
9 distribution is also acceptable for organic matter ( $p = 0.57$ ). The Kruskal-Wallis test showed  
10 significant differences at the 10% level in terms of land use ( $p = 0.08$ ) but not in terms of  
11 (SCU) ( $p = 0.17$ ).

12 Table II also provides the shape parameters of the retention and hydraulic conductivity curves  
13  $n$  and  $\eta$ . The  $n$  parameter should be larger than two so that  $m$  derived from Eq.(3) is positive.  
14 The average value of  $n$  (2.17) is therefore quite low and its variability is small (CV of about  
15 152%). The  $\eta$  parameter has a mean value of 15.2 and a higher coefficient of variation (20%).  
16 The Gaussian distribution was found acceptable for  $n$  at the 5% level ( $p = 0.07$ ), and  $\eta$  at the  
17 10% level ( $p = 0.12$ ). The  $n$  and  $\eta$  parameters have small coefficient of variations and the  
18 average value can be considered as representative of the catchment. However, this hypothesis  
19 must be verified using the distributed hydrological model. These parameters control the decay  
20 of the retention and hydraulic conductivity curves when the soil dries out, through a power  
21 function. And some authors have reported a high sensitivity of water balance components to  
22 small variations of  $n$  (e.g. Braud, 1998; Boulet *et al.*, 1999).

### 23 *Dry bulk density and porosity*

24 The dry bulk density estimated using the 0-2.5 cm height and the 0-5 cm height cylinders are  
25 compared in Figure 5a. The correlation is good,  $R^2 = 0.85$  ( $p < 10^{-6}$ , 19 samples), with values of

2

16

1

1the dry bulk density in general lower when using the smaller cylinders. This result is not  
2surprising as the 0-2.5 cm height samples consist almost exclusively of topsoil which contains  
3more organic matter and vegetation residues. The average dry bulk density of all the samples  
4was  $1078 \text{ kg m}^{-3}$  ( $\pm 318$ ). This value is quite low. Soil 704, classified as loamy sand to clayey  
5sand presents the highest density of  $1330 \text{ kg m}^{-3}$  ( $\pm 281$ ). In contrast soil 1031 (loamy sand  
6from tuffs) shows the lowest average of  $709 \text{ kg m}^{-3}$  ( $\pm 135$ ).

7The statistics of the 0-5 cm height values with respect to land use classes are presented in  
8Table III, as well as the statistics of organic matter and porosity (see also Figure 3b). As  
9expected, the highest organic matter contents are observed in permanent pasture and forest  
10soils whereas the lowest values are encountered in the cultivated fields. Points with the  
11highest organic matter content are associated with the lowest dry bulk density and highest  
12porosity. This is illustrated in Figure 5b which shows the correlation between dry bulk density  
13and organic matter content. The correlation is significant with  $R^2=0.54$  ( $p = 10^{-5}$ , 27 samples).

14

15The statistics of organic matter and dry bulk density with respect to pedologic units (SCU) are  
16not shown in Table III as the Kruskal-Wallis test indicated that differences amongst classes  
17were not significant at the 10% level ( $p=0.18$ ) when soil 1031, exhibiting the lowest values,  
18was excluded. The differences in terms of land use were significant. The Wilcoxon rank sum  
19test (or Mann-Witney test) was performed for all the combinations of two land use groups. It  
20allowed the proposition of three main classes of dry bulk density by gathering the classes  
21where the  $p$ -value was higher than 0.1. One class could be identified easily corresponding to  
22forest soils (broad leaved and coniferous forests) with the lowest dry bulk density and highest  
23organic matter content (class DB1). For the two other classes, it was not so easy to distinguish  
24between land uses, especially for land use 4 (bare soil after ploughing). Based on the largest  $p$   
25values, we defined the two other classes as follows: permanent pasture, clearing and small

1

1 woods for class DB2, with intermediate dry bulk density; and cultivated pasture, crops and  
2 orchards for class DB3 with the highest dry bulk density. The statistical properties of the  
3 variables with respect to these new classes are presented in Table IV. We verified *a posteriori*  
4 that the classification was relevant, as the  $p$  value amongst any pair of classes was lower than  
5  $10^{-6}$ . A cluster analysis of the points, described using dry bulk density and organic matter  
6 content, led to the same three main classes as the method presented above. It strengthens the  
7 conclusion that land use has a strong impact on the topsoil dry bulk density. This can be  
8 explained by agricultural practices and machines that induce a higher dry bulk density  
9 corresponding to a soil compaction.

10 The same classes are obtained for porosity, as the latter is a decreasing function of the dry bulk  
11 density.

12 We mentioned before that the final water content  $\theta_0$  was assumed to be equal to the saturated  
13 water content. To assess the consistency of this hypothesis, we calculated the ratio  $\theta_0/\varepsilon$ . Three  
14 points had values higher than 1 and the final water content was thus set to the porosity. The  
15 range of the values was large: [0.35-1]. Values lower than 0.4 were associated to forest or  
16 small woods soils with a high organic matter content and a high porosity. The hydrophobic  
17 effect of organic matter could also influence these results. The average of the ratio was  $0.7 \pm$   
18  $0.18$  (57 points), a value much lower than the values commonly reported in the literature 0.8-1  
19 (Rogowski, 1971). Table IV shows the values of this ratio per dry bulk density classes (DB1,  
20 DB2 and DB3). It shows a large range of values for the three classes with a range of [0.3-1.0]  
21 in all cases. Contrary to what happens for dry bulk density and porosity, the differences  
22 amongst the three classes are not significant for this ratio with values of the Wilcoxon rank  
23 sum test  $p$ -values larger than 0.65.

1

1

## 2 *Fitting of single ring and mini-disk infiltration tests*

3 Due to the experimental protocol (small oscillations of the water surface just after removing  
4 the plastic sheet), there were some uncertainties on the initial level within the cylinder.  
5 Furthermore, due to the terrain slope (from zero to about 10%), the initial value was not  
6 always equal to the nominal value corresponding to the water volume divided by the cylinder  
7 surface, i.e. 95.5 mm. The initial level was thus adjusted manually to ensure data consistency.  
8 In order to assess *a posteriori* the reliability of the fitted parameters for the two methods, we  
9 calculated the gravitational time given by Eq. (9). For 76% of the SR infiltration test and 65%  
10 of the MDI tests, the total infiltration time was larger than the gravitational time. Thus the  
11 asymptotic regime could be assessed with a good accuracy for these tests and all the data were  
12 processed using both Eq. (6) and Eq. (10). On the other hand, the short time infiltration Eq.  
13 (6) could be valid for only a very few points, leading to less robust estimation of sorptivity.  
14 This is illustrated on Figure 6a where only the 6 first data points fit the short time model and  
15 the other points fit the asymptotic equation. In this case, the influence of capillary force was  
16 very short and the gravitational time was reached after about 100 s. In this case, the sorptivity  
17 was estimated with only a small number of points which can be detrimental to the robustness  
18 of the optimization, but is theoretically adequate. When the maximum infiltration time was  
19 lower than the gravitational time, the short time model of Eq. (6) was valid for the whole  
20 infiltration test duration. In this case, the estimated sorptivity was numerically robust, whereas  
21 the estimation of the asymptotic regime was less easy. This is illustrated in Figure 6b where  
22 the slope of the long time infiltration curve (Eq.(10)) is parallel to the asymptotic infiltration  
23 equation (dashed line) and the data fit the short time model up to the end. It shows that the  
24 gravitational time was not yet reached. For these infiltration tests, the effect of the terrain  
25 slope on the results was thus minimum and the estimation of sorptivity was robust (Chen and

1

1Young, 2006). Figure 6 illustrates the SR data but the same kind of results was obtained for  
2the mini-disk infiltration data.

3For the SR infiltration tests, the average gravitational time was  $6 \text{ min} \pm 14 \text{ min}$  and, for the  
4MDI infiltration tests, the average was  $60 \text{ min} \pm 138 \text{ min}$ . It can be compared to the  
5infiltration test duration which was  $10 \text{ min} \pm 19 \text{ min}$  for SR and  $33 \text{ min} \pm 35 \text{ min}$  for the MDI  
6infiltration tests. Capillary effects were thus very short for the positive head infiltration tests,  
7whereas they lasted much longer for tension-disk infiltration. In both cases however, the use  
8of the BEST method for optimization allowed to exploit at best the available data both before  
9and after the gravitational time was reached.

10

### 11 *Single ring infiltration tests*

12Table V shows the results of the infiltrated depth and maximum infiltration time. The values  
13show that the infiltrated depth was close to the nominal value (volume of water / cylinder  
14surface = 95.5 mm) with a median of 90 mm. Only four points did not work very well and had  
15a much smaller infiltration depth. The slope of the terrain over which the cylinders were  
16installed was responsible for this difference between the real and nominal infiltrated depths.  
17In terms of maximum infiltration time, the range was from a few seconds (15 s) to 114 min  
18for the longest test, with an average value of about 10 min and a median of about 3 min. Thus  
19half of the infiltration tests took place in less than 3 min, which was very rapid and allowed to  
20minimize the possible effect of slope on the infiltration. The high infiltration rates can also be  
21related with preferential flow, which is not sensitive to slope effect. Only three tests had  
22duration larger than 45 min, and two of them were located on flat areas.

23As in de Condappa (2005), we introduce the ratio

$$24 \quad L = I_{\max} / t_{\max} \quad (15)$$

2

20

1

1 where  $I_{max}$  (mm) is the maximum infiltrated depth and  $t_{max}$  (s) is the time to infiltrate this  
2 quantity. As all the infiltration tests had about the same maximum infiltrated quantity, this  
3 ratio could be used to rank the infiltration tests in terms of “infiltration capacity”. The  
4 corresponding statistics are also provided in Table V. The average value is about  $56 \text{ mm min}^{-1}$   
5 and the median  $27 \text{ mm min}^{-1}$ . These values show very high infiltration capacity for the  
6 catchment.

7 The statistics of estimated sorptivity and saturated hydraulic conductivity are provided in  
8 Table III categorized in terms of land use. As for dry bulk density, differences in  $K_s$  were not  
9 found significant in terms of pedology, with a value of the Kruskal-Wallis test of  $p=0.14$ .  
10 Significant differences were found in terms of land use. Three main classes could be  
11 identified (Figure 7). One class, class KS1, could be distinguished clearly. It was composed of  
12 land use 6 and 9 (broad leaved forest and small woods) with the highest saturated hydraulic  
13 conductivity and sorptivity (Table VI). The other land use classes could not be distinguished  
14 so easily and were defined based on the largest  $p$  values. Class KS2 includes land uses 2, 4,  
15 and 7 (cultivated pasture, bare soil after ploughing and clearing) with the lowest saturated  
16 hydraulic conductivity and sorptivity (Table VI). Finally class KS3 contains the other land  
17 uses (1, 3, 5, 8), namely permanent pasture, crops – wheat stubble and orchards-, and  
18 coniferous forest, with intermediate saturated hydraulic conductivity (Table VI). We verified  
19 *a posteriori* that the differences in distribution remained significant for both variables with the  
20 new classes with  $p$ -values of the Wilcoxon rank sum test lower than 0.006. Table VI also  
21 provides the statistics of the  $h_{VG}$  parameter. No significant differences amongst land use  
22 classes was found for  $h_{VG}$  with  $p$ -value of the Wilcoxon-test larger than 0.2. The value for  $h_{VG}$   
23 is then considered as the same for all the KS and DB classes.

24 The classes in terms of saturated hydraulic conductivity are different from the classes  
25 identified for dry bulk density. In particular, coniferous forest and broad leaved forests were

1

1 in the same group for dry bulk density. It is not the case for saturated hydraulic conductivity,  
2 which shows that organic matter content and dry bulk density are not the only factors  
3 influencing  $K_s$ .

4

#### 5 *Tension-disk infiltration tests and comparison between the two methods*

6 At first, data analysis was conducted using traditional methods as described in Smiles and  
7 Knight (1976) or Vandervaere et al. (2000a). These methods fit only the short to medium time  
8 infiltration model of Eq. (6) and only a small amount of the data could be used. The  
9 estimation was not robust and mostly produced negative hydraulic conductivity values. This  
10 was not surprising, given the small cylinder radius and short transient stage of infiltration.  
11 Indeed, Vandervaere et al. (2000b) showed that, in these experimental conditions, their ST  
12 (single test) method was not recommended. The results are therefore not discussed below. We  
13 saw that the BEST method uses the whole infiltration test data, including the asymptotic  
14 regime. It allowed the derivation of reliable sorptivity and hydraulic conductivity estimates  
15 for 39/43 MDI infiltration tests. The rejected tests were in general conducted in forest or  
16 permanent pasture, where the impact of macropores might have been large and where the size  
17 of the apparatus (45 mm in diameter) did not allow aggregation of the soil heterogeneity.  
18 Table VI presents the statistics of the parameters derived from the mini-disk infiltrometer for  
19 the three classes identified for saturated hydraulic conditions. As expected, sorptivity and  
20 hydraulic conductivity were larger for the SR than for the MDI infiltration tests. The  
21 Wilcoxon rank sum tests showed that differences in distribution amongst KS classes was not  
22 significant for sorptivity and only significant for class KS3 for hydraulic conductivity. The  
23 impact of land use change on hydraulic properties was thus most pronounced at saturation.  
24 Table VI also provides the ratio between  $K_s$  and  $K(-20\text{ mm})$ . The most striking result was the  
25 sharp increase of hydraulic conductivity from near saturation (-20 mm of water pressure) to

2

22

1

1saturation with a ratio between the averages larger than 500, and a ratio between the median  
2of 46.

3

#### 4Retention and hydraulic conductivity curves

5All the results presented in the paper can be summarized by showing the retention and  
6hydraulic conductivity curves typical for the combination of the DB and KS land use classes.  
7They are shown in Figure 8 where average values of shape parameters from Table II, average  
8values of saturated water content (calculated as average porosity times average  $\theta_s/\varepsilon$  ratio)  
9from Table IV and averages values of  $h_{VG}$ ,  $K_s$  and  $K(-20\text{ mm})$  in Table VI were used. The three  
10retention curves differ mainly in saturated water content, as the same values of  $h_{VG}$  and  $n$  are  
11used and each curve is associated with one of the DB classes. For the hydraulic conductivity  
12curves, the Brooks and Corey model (Eq. (4)) was applied for water content lower than the  
13value at  $h=-20$  mm. Between this value and saturation a linear relationship between the  
14natural logarithm of conductivity versus water content was assumed, as previously done to  
15take into account the effect of macropores (Olioso *et al.*, 2002). A more comprehensive  
16model, as the one proposed by Jarvis (2009) could be also be used to represent the sharp  
17increase in hydraulic conductivity when moving from near-saturation to saturation.  
18Then one curve should be drawn for the various possible combinations of DB and KS classes.  
19Below -20 mm for  $h$ , and the corresponding value for  $\theta$ , the curves  $K(\theta)$  differ only due to  
20differences in saturated water contents – the same value is used for the parameter  $\eta$  and there  
21are only small differences between  $K(-20\text{mm})$  for a given DB class -. Therefore, only three  
22curves can be distinguished, that correspond mainly to the DB classes, Between -20 mm of  
23pressure and the saturation, the  $K(\theta)$  curves differ also because of differences in the saturated



1

1hydraulic conductivity values  $K_s$ . Briefly, the water retention curve are only DB classes  
2dependent and the hydraulic conductivity  $K(\theta)$  are both DB and KS classes dependent.

3The differences in saturated hydraulic conductivities identified amongst land use are only  
4influential on a small part of the curves, i.e very close to saturation. The accurate  
5determination of saturated water content (and therefore of dry bulk density) is shown to be the  
6most important point to get accurate description of soil hydraulic properties over the whole  
7range of water content. As we have shown that dry bulk density is highly related to organic  
8matter content, these differences can be assessed quite easily in the field.

9

#### 10*Mapping of topsoil hydraulic properties*

11From the results presented previously, a preliminary mapping of topsoil hydraulic properties  
12over the Mercier catchment can be proposed.

13In our case study, we have shown that the soil texture is quite homogeneous and that the  
14variability of the shape parameters of the retention and hydraulic conductivity curves,  $n$  and  
15 $\eta$ , is low. As a first approximation, these parameters are assumed constant over the whole  
16catchment. A more refined map could be obtained by mapping first the clay, sand, and silt  
17contents, using for instance the kriging technique. The shape parameters  $n$  and  $\eta$  could then  
18be derived from the soil texture, as done in this paper (see also Lassabatère *et al.*, 2006).

19The major outcome of our study is to show that soil porosity, saturated water content and  
20saturated hydraulic conductivity, are mostly determined by land use. A land use map can  
21therefore be used for the mapping of those parameters. In our study catchment, the land use  
22field survey has shown that the accuracy of the Corine land cover map was too low to  
23properly distinguish between the relevant land uses, especially crops. A more detailed land  
24use map is therefore required. It can be derived from high resolution aerial photographs or  
25satellite imagery. Such mapping is in progress on the Yzeron catchment (Béal *et al.*, 2009) but

2

24

1

1 was not available at the time of the field survey. For the Mercier catchment, a detailed map  
2 was digitalized from aerial photographs (IGN BD ORTHO 2003, updated using the IGN BD  
3 ORTHO 2008) and corrected using the cadastre for urbanised areas. This map was  
4 reclassified for the representation of topsoil hydraulic properties. This classification combines  
5 the DB classes of Table IV and the KS classes of Table VI. The correspondence between the  
6 original land use map and the reclassified one is given in Table VII. The resulting map is  
7 shown in Figure 9 where non sampled areas appear in white colour. For each DB-KS class,  
8 one value of porosity, saturated water content and hydraulic conductivity can be affected  
9 using for instance the average of the DB classes and the media of the KS classes (Table VII).

10

## 11 DISCUSSION

12

### 13 *Sampling strategy*

14 The sampling strategy is very important for an efficient mapping of the hydraulic parameters.  
15 It has been pointed out as a key question by Park and van de Giesen (2004). The question of  
16 sampling is especially relevant when dealing with a large catchment such as the Mercier  
17 catchment (7 km<sup>2</sup>) (published studies are often related to catchments of less than 1 km<sup>2</sup>). In  
18 previous works performed using the *Beerkan* method, on much larger catchments, a regular  
19 grid sampling was used. Such a strategy was used during the EFEDA project on a 10x10 km<sup>2</sup>  
20 area in Central Spain (Braud *et al.*, 2003). A regular grid (3.5 km resolution) complemented  
21 by a transect with a 20 m spacing, was also used during a field campaign conducted in the  
22 Donga catchment (580 km<sup>2</sup>) in Benin (Varado *et al.*, 2006). Analysis of the Benin data  
23 showed a spatial correlation of about 50 to 100 m for the saturated hydraulic conductivity and  
24 no correlation on the 3.5 km grid. On the other hand, it was shown that average values were  
25 significantly different when the data were classified according to pedological units. A regular

1

1grid sampling does not allow the valorization of existing information such as pedology and  
2land use. The sampling strategy adopted in this study was focused on the future hydrological  
3modeling, where the hydrological units, coined as hydro-landscapes by Dehotin and Braud  
4(2008), are chosen to be as homogeneous as possible with respect to soil, land use and other  
5factors such as slope or the Beven topographic index. The pre-selection of sites based on the  
6combination of pedology and land use information, as well as accessibility, was found  
7efficient in terms of duration of the field campaign and use of human resources. It allowed the  
8sampling of pedology/land use combinations representing a significant fraction of the  
9catchment area. As shown in Figure 9, the characterization of artificialized areas is missing,  
10but lots of practical problems (mainly difficult access to private properties) prevent an  
11efficient sampling of these areas. As much as possible, the literature should be used instead.

### 12*Results of the infiltration tests*

13In this study two types of infiltration test were used to assess the hydraulic properties of the  
14Mercier catchment topsoil A horizon. For a given location, the results of the three SR  
15infiltration tests replications were in general very consistent whereas the variability was larger  
16for the MDI infiltration tests. The difference in sampling surface between both devices may  
17be the explanation. Indeed, the large cylinder diameter of the SR tests averaged most of the  
18soil heterogeneity and removed much of the spatial variability due to inadequate sampling of  
19macropore effect. The large diameter of the cylinder also filtered out the effects of terrain  
20slope and vegetation. It reduces the effect of the heterogeneity of soil structure and texture  
21and the parameters estimated from the infiltration tests are associated with this weighing of  
22surface heterogeneities. The obtained values can therefore be considered representative of the  
23field. On the other hand, the sampling surface of the MDI infiltrometer was very small and  
24therefore these were much more sensitive to soil variability and heterogeneity of the topsoil A  
25horizon. However, given the slope and the surface heterogeneity, it would have been difficult

1

1to use a large diameter for the mini-disk: this apparatus requires a flat surface to ensure  
2stability and a good contact with the membrane. This would have required digging through  
3the slope, that would have disturbed the soil surface and would not have been representative  
4of the topsoil anymore. Finally, the two types of infiltration tests were complementary and  
5well adapted to the field conditions on this highly structured soil.

6In addition, the positive head infiltration test allowed a characterization of saturated  
7conditions, whereas the tension-disk data provided information on near-saturated hydraulic  
8conductivity (-20 mm of water pressure), and illustrated the sharp increase in conductivity  
9when moving from near-saturated to saturated conditions. This difference can be explained by  
10the activation, at saturation, of a macropore network related to the high organic content, and a  
11higher root system density and soil fauna activity in natural vegetations (broad leaved forest,  
12permanent pasture). A review of the effect of macropores on water flow has been proposed by  
13Beven and Germann (1982). They reports an increase of the infiltration capacity of soils with  
14macropores. In the paper by Zhou *et al.* (2008, Table 5, Fig. 1), a ratio of about 10 between  
15hydraulic conductivity at -30 mm of pressure and saturation is reported for woodland,  
16cropland, pasture and urban land uses. In the paper by Schwartz *et al.* (2003, Fig. 3) the ratio  
17between hydraulic conductivity at -20 mm of pressure and saturation is of about 2. In these  
18two papers saturated hydraulic conductivity was obtained using tension-disk infiltrometers  
19with a pressure of 0 m, which are shown by Reynolds *et al.* (2000) to provide lower estimates  
20of saturated hydraulic conductivity than pressure infiltrometers Our values are therefore  
21consistent with the literature, although the values of the ratio is around 50 in our study.

22

23The BEST method used in data interpretation was found robust and allowed us to obtain  
24results even in adverse conditions (gentle slope, very rapid infiltration, and dense vegetation  
25detritus cover in some cases). The strength of the method is its ability to exploit both the short

1

land long term ranges of the infiltration tests in order to describe at best the data. It also  
2provided physical results when traditional methods, based only on the short time infiltration  
3regime, failed. The method is applicable for both positive head and tension-disk infiltration  
4data, provided the contact layer has no significant influence on the early stages of infiltration.  
5When positive head is applied, the method provides an estimate of the normalization  
6parameter for the pressure and thus a complete description of both the retention and hydraulic  
7conductivity curves, which is not the case of traditional analysis methods. However, several  
8limitations of the methods have been identified. Xu et al. (2009) underline that the BEST  
9method is not effective when the initial water content is not sufficiently different from the  
10final water content. However, this restriction apply to all the methods of analysis because the  
11difference in water content appears in the denominator of Eq. (6). Another limitation is related  
12to the use of two different equations during the analysis which requires the determination of  
13the number of points where the small time infiltration equation is valid, through a specific  
14BEST routine (Eq. (7)). This choice influences the final sorptivity value and is therefore  
15important. The approximation provided by Eq.(6) was shown to be adequate for modeling  
16Beerkan infiltration experiments, provided its use is restricted to valid intervals (Lassabatere  
17et al., 2009). Improvement of the BEST method were recently proposed for specific soils  
18(Yilmaz et al., 2010) but were not used here. Based on the validation of the full integration  
19equation (Lassabatere et al., 2009), work is in progress in order to directly solve the full  
20infiltration equation proposed by Haverkamp et al. (1994). The results presented in the paper  
21were partly verified using this new solution, which strengthens the confidence in the  
22conclusions. More theoretical and numerical studies should be conducted to better assess the  
23impact of slope on the final results.

### *1 Impact of land use on topsoil hydraulic properties*

2 Our study also highlighted the impact of land use on soil structural parameters, whereas the  
3 impact of pedology was not found so significant in our case study. Three land use classes  
4 were identified, leading to significant differences in dry bulk density and porosity. These  
5 classes were highly related to the organic matter content and therefore to the land use insofar  
6 as organic matter content is lower in cultivated lands than in natural areas (forests, permanent  
7 pastures). Lal (1996) reported an increase in dry bulk density when forest was replaced by  
8 cultivated lands, which is consistent with our findings.

9 In our study, three further land use classes were identified with significant differences in  
10 saturated hydraulic conductivity and sorptivity. However, these classes were not significantly  
11 different in terms of near-saturated hydraulic conductivity, showing that the classes were  
12 probably related to macropores. Once again, the appearance of a dense macropore network is  
13 favoured by fauna activity and the dense root network in natural vegetations. Several authors  
14 have reported results showing the impact of land use on soil hydraulic properties. For  
15 instance, Marshall *et al.* (2009) report higher saturated hydraulic conductivity of soil beneath  
16 tree hedges than in agricultural fields, with a ratio of the both of about 3. Reynolds *et al.*  
17 (2000, Table 4) report values of saturated hydraulic conductivity measured using pressure  
18 infiltrometers. The geometric mean values on natural woodlot are 2 to 10 times larger than  
19 those under conventional and no-tillage practices. More stable soil structure and increased  
20 biological activity might explain the larger hydraulic conductivity in forest, permanent pasture  
21 or minimum tillage systems (Bodhinayake and Si, 2004). Stolte *et al.* (2003) report that the  
22 permanent land use (forest, orchard, wasteland, shrub) showed a greater heterogeneity of  
23 saturated hydraulic conductivity than the arable areas and the values were significantly higher  
24 in permanent land use than in cultivated areas, as in our study. This was probably due to more  
25 macropores, associated with the activity of fauna and roots in the permanent system than in

1

1arable land. Such changes in topsoil hydraulic properties are very important for hydrological  
2processes such as surface runoff but also groundwater, and water quality. They modify the  
3hydrological response in terms of water balance components and their annual temporal  
4variability (e.g., Fohrer *et al.*, 2005; Bormann *et al.*, 2007). Hibbert (1967) and Bosch and  
5Hewlett (1982) concluded that a reduction of the forest cover increases water runoff.

6Our data were collected in autumn, but especially for agricultural fields, our results should be  
7complemented by a monitoring of the time evolution of soil hydraulic properties, as suggested  
8by several studies. This fact is especially relevant for agricultural fields where soil properties  
9are modified regularly by agricultural practices such as ploughing, sowing, etc...(Zhou *et al.*,  
102008; Bormann and Klassen, 2008; Le Bissonais *et al.*, 2005; Schwarts *et al.*, 2003; Mubarak  
11*et al.*, 2009).

12

## 13CONCLUSIONS

14The results presented in this paper show that using an adequate spatial sampling taking into  
15account pedology, and especially land use, it was possible to document the spatial variability  
16of soil hydraulic properties of a small catchment of 7 km<sup>2</sup>. The use of two types of infiltration  
17tests, namely positive head and tension disk infiltration tests, combined with particle size data  
18analysis and porosity measurements, allowed the derivation of estimates of the retention and  
19hydraulic conductivity curves. Positive head and tension-disk data provided complementary  
20information about saturated and near-saturated hydraulic conductivity of the topsoil A  
21horizon. They highlighted a sharp increase of hydraulic conductivity when moving from  
22near-saturated (-20 mm of water pressure) to saturated conditions. This fact could be related  
23to the existence of macroporosity, mainly related to land use management. Therefore, the  
24monitoring of both saturated and near-saturated hydraulic conductivity can provide  
25information on the long term impact of land use on soil hydraulic properties.

1

In addition, the study revealed a significant impact of land use on dry bulk density and porosity, as well as on saturated hydraulic conductivity. This result opens perspectives for the spatialization of soil hydraulic conductivity. Traditionally, in distributed hydrological models, soil hydraulic properties are specified using pedo-transfer functions that rely mainly on soil texture and sometimes on porosity (or dry bulk density). These functions are generally fitted on a limited data set, often obtained in the laboratory, and might not be adapted to *in situ* soil conditions. Our study highlights the impact of land use on soil hydraulic properties and confirms the results of other authors such as those mentioned in the *Discussion* section. This should also be taken into account in the mapping of soil hydraulic properties for hydrological modelling. We have shown that a high resolution land use map is very valuable and can be used for this purpose.

12

### 13ACKNOWLEDGEMENTS

The soil data base was provided by SOL INFO RHONE-ALPES, [sira@rhone-alpes.chambagri.fr](mailto:sira@rhone-alpes.chambagri.fr), <http://www.rhone-alpes.chambagri.fr/sira/>. The study was funded by the French Agence Nationale de la Recherche (ANR) under contract n° ANR-07-VULN-1701. The stay of the first author at Cemagref was funded by Queretaro University, Mexico and Cemagref. Jean-Pierre Vandervaere provided useful comments on the interpretation of tension disk infiltration tests. We also thank two anonymous reviewers for their suggestions which help improve the quality of the paper.

21

### 22REFERENCES

Béal D, Gagnage M, Jacqueminet C, Kermadi S, Michel C, Jankowsky S, Branger F, Braud I. 2009. Cartographie de l'occupation du sol pour la modélisation hydrologique spatialisée du



1

1cycle de l'eau en zone péri-urbaine, Proceedings 2<sup>ème</sup> atelier SIDE2009 Systèmes  
2d'Informations et de Décision pour l'Environnement, Biramonte S, Miralles A, Pinet F (eds),  
3Toulouse, France, May 26 2009, 10 pp. Available at [http://eric.univ-](http://eric.univ-lyon2.fr/~sbimonte/side2009.html)  
4[lyon2.fr/~sbimonte/side2009.html](http://eric.univ-lyon2.fr/~sbimonte/side2009.html), consulted on 2010/01/15.

5Beven K, Germann P. 1982. Macropores and water flow in soils. *Water Resources Research*,  
6**18(5)**: 1311-1325.

7Bodhinayake W, Si BC. 2004. Near-Saturated surface soil hydraulic properties under different  
8land use in the St Denis National Wildlife Area, Saskathchewan, Canada. *Hydrological*  
9*Processes* **18**: 2835-2850.

10Booth DB, Hartley D, Jackson R. 2002. Forest cover, impervious-surface area, and the  
11mitigation of stormwater impacts. *Journal of the American Water Resources Association*,  
12**38(3)**: 8356-845.

13Bormann H, Breuer L, Gräff T, Huisman JA. 2007. Analysing the effects of soil properties  
14changes associated with land use changes on the simulated water balance: A comparison of  
15three hydrological catchment models for scenario analysis. *Ecological Modelling*, **209(1)**: 29-  
1640.

17Bormann H, Klassen K. 2008. Seasonal and land use dependent variability of soil hydraulic  
18and soil hydrological properties of two Northern German soils. *Geoderma* **145**: 295-302.

19Bosch JM, Hewlett PM. 1982. A review of catchment experiments to determine the effect of  
20vegetation changes on water yield and evapotranspiration. *Journal of Hydrology* **55**:3-23.

21Boulet G, Kalma JD, Braud I, Vauclin M. 1999. An assessment of effective parameterization  
22of soil physical and land surface properties in regional-scale water balance studies. *Journal of*  
23*Hydrology* **217**: 225-238.

24Bras RL, Perkins FE. 1975. Effects of urbanization on catchment response. *J. of Hydraulics*  
25*Division* **101** HY3: 451-466.

2

32

1

1Braud I. 1998. Spatial variability of surface properties and estimation of surface fluxes of a  
2savannah. *Agricultural and Forest Meteorology* **89(1)**: 15-44.

3Braud I, de Condappa D, Soria J, Haverkamp R, Angulo-Jaramillo R, Galle S, Vauclin M.  
42005. Use of scaled forms of the infiltration equation for the estimation of unsaturated soil  
5hydraulic properties (Beerkan method). *European Journal of Soil Science* **56**: 361-374. DOI:  
610.1111/j.1365\_2389.2004.00660.x.

7Braud I, Haverkamp R, Arrué JL, Lopez MV. 2003. Spatial variability of soil surface  
8properties and consequences on the annual and monthly water balance of a semi-arid  
9environment (EFEDA experiment). *Journal of Hydrometeorology* **4(1)**: 121-137.

10Brooks RH, Corey CT. 1964. Hydraulic properties of porous media. *Hydrological Paper* **3**.  
11Colorado State University, Fort Collins, CO.

12Burdine NT. 1953. Relative permeability calculations from pore size distribution data.  
13*Transactions of the American Institute of Mining, Metallurgical, and Petroleum Engineers*  
14**198**: 71-77.

15Chen L, Young MH. 2006. Green-Ampt infiltration model for sloping surfaces. *Water*  
16*Resources Research* **42**: W07420, doi:10.1029/2005WR004468

17Childs EC, Collis-George C. 1950. The permeability of porous media. *Proceedings of the*  
18*Royal Society London Series A* **201**: 393-405.

19Chocat B, Krebs P, Marsalek J, Rauch W, Schilling W. 2001. Urban drainage redefined: from  
20stormwater removal to integrated management. *Water and Science Technology* **43**:61-68.

21Clapp RB, Hornberger GM. 1978. Empirical equations for some soil hydraulic properties.  
22*Water Resources Research* **14(4)**: 601-604.

23Cosby BJ, Hornberger, GM, Clapp RB, Ginn TR. 1984. A statistical exploration of the  
24relationships of soil moisture characteristics to the physical properties of soils. *Water*  
25*Resources Research* **20(6)**: 682-690.

1

1de Condappa D. 2005. Etude de l'écoulement d'eau à travers la zone non-saturée des aquifères  
2de socle à l'échelle spatiale du bassin versant. Application à l'évaluation de la recharge au sein  
3du bassin versant de Maheshwaram, Andhra Pradesh, Inde, Université Joseph Fourier,  
4Grenoble, France, 22 Avril 2005, 355 pp.

5de Souza ES, Antonino ACD, Angulo-Jaramillo RA, Netto AM, Montenegro SMGL, da Silva  
6EB. 2008. Spatial variability of hydrodynamic parameters in two agricultural plots in Paraíba  
7state – Brazil, *Reivista, Brasileira de ciencia do solo* **32(5)**: 1795-1804.

8Dehotin J, Braud I. 2008. Which spatial discretization for distributed hydrological models?  
9Proposition of a methodology and illustration for medium to large scale catchments.  
10*Hydrology and Earth System Sciences* **12**: 769-796.

11Desbordes M. 1989. Principales causes d'aggravation des dommages dus aux inondation par  
12ruissellement superficiel en milieu urbanisé. *Bulletin hydrologie urbaine- SHF*, Paris, **4** : 2-  
1310.

14Fohrer N, Haverkhamp S, Frede H. 2005. Assessment of the effects of land use patterns on  
15hydrological landscape functions: development of sustainable land use for low mountain  
16range areas. *Hydrological Processes* **19** : 659-672.

17Gnouma R. 2006. Aide à la calibration d'une modèle hydrologique distribué au moyene d'une  
18analyse des processus hydrologiques: application au bassin versant de l'Yzeron. Thèse  
19Doctoral. Institut National des Sciences Appliquées de Lyon. France, 412 pp.

20Gutmann ED, Small EE. 2005. The effect of soil hydraulic properties versus soil texture in land  
21surface models. *Geophysical Research Letters* **32**: L02402, doi: 10.1029/2004GL021843.

22Haverkamp R, Bouraoui F, Angulo-Jaramillo R, Zammit C, Delleur JW. 1998. Soil properties  
23and moisture movement in the unsaturated zone. In: *CRC Groundwater Engineering*  
24*Handbook*, Delleur JW (ed), CRC Press, Boca Raton, Florida: 5.1-5.50,.

1

- 1Haverkamp R, Leij FJ, Fuentes C, Sciortino A, Ross PJ. 2005. Soil water retention: I.  
2Introduction of a shape index. *Soil Science Society of America Journal* **69**: 1881-1890, doi:  
310.2136/sssaj2004.0225.
- 4Haverkamp R, Ross PJ, Smettem KRJ, Parlange JY. 1994. Three-dimensional analysis of  
5infiltration from the disk infiltrometer 2. Physically based infiltration equation. *Water*  
6*Resources Research* **30(11)**: 2931-2935.
- 7Herman S, Mertens J, Timmerman A, Feyen J. 2003. Comparison of tension infiltrometer,  
8single-ring pressure infiltrometer and soil core Ksat estimates on a sandy loam hillslope. EGS  
9- AGU - EUG Joint Assembly, Abstracts from the meeting held in Nice, France, 6 - 11 April
- 10Hibbert AR. 1967. Forest treatment effects on water yield. In the International Symposium  
11on Forest Hydrology, Pennsylvania , September 1965, Sopper WE, Lull HW (eds.) Pergamon;  
12Oxford.
- 13Islam N, Wallender WW, Mitchell JP, Wicks S, Howitt RE. 2006. Performance evaluation of  
14methods for the estimation of soil hydraulic parameters and their suitability in a hydrologic  
15model. *Geoderma* **134(1-2)**: 135-151.
- 16Jarvis N. 2009. Near-saturated hydraulic properties of macroporous soils. *Vadose Zone*  
17*Journal* **7**: 1302-1310.
- 18Lafont M, Vivier A, Nogueira S, Namour P, Breil P. 2006. Surface and hyporheic oligochaete  
19assemblages in a French suburban stream. *Hydrobiologia* **564(1)**: 183-193.
- 20Lal R. 1996. Deforestation and land-use effects on soil degradation and rehabilitation in  
21western Nigeria. I. Soil physical and hydrological properties. *Land degradation and*  
22*development* **7**: 19-45.
- 23Lassabatère L, Angulo-Jaramillo R, Soria Ugalde JM, Cuenca R, Braud I, Haverkamp R.  
242006. Beerkan estimation of soil transfer parameters through infiltration experiments. *Soil*  
25*Science Society of America Journal* **70**: 521-532.

1

- 1Lassabatère L, Angulo-Jaramillo R, Soria Ugalde JM, Simunek J, Haverkamp R. 2009.  
2Analytical and numerical modeling of water infiltration experiments. *Water Resources*  
3*Research* **45**: W12415.
- 4Le Bissonnais Y, Cerdan O, Lecomte V, Benkhadra H, Souchere V, Martin P. 2005.  
5Variability of soil surface characteristics influencing runoff and interrill erosion. *Catena* **62**:  
6111-124.
- 7Marsalek J, Jiménez-Cisneros BE, Karamouz M, Malmquist PA, Gldenfum J, Chocat B.  
82007. Urban water processes and interactions. UNESCO IHP-VI program, UNESCO, Paris,  
9239 pp.
- 10Marshall MR, Francis OJ, Frobrook ZL, Jackson BM, McIntyre N, Reynolds B, Solloway I,  
11Weather HS, Chell J. 2009. The impact of upland land management on flooding: results from  
12an improved pasture hillslope. *Hydrological Processes* **23**: 464-474.
- 13Matteo M, Randhir T, Bloniarz D. 2006. Watershed-scale impacts of forest buffers on water  
14quality and runoff in urbanizing environment. *Journal of the American Water Resources*  
15*Association* **132**:144-152.
- 16Mualem Y. 1976. A new model for predicting the hydraulic conductivity of unsaturated  
17porous media. *Water Resources Research* **12**, 513-522.
- 18Mubarak I, Mailhol JC, Angulo-Jaramillo R, Ruelle P, Khaledian M. 2009. Temporal  
19variability in soil hydraulic properties under drip irrigation. *Geoderma* **150(1-2)**: 158-165  
20doi:10.1016/j.geoderma.2009.01.022.
- 21Oliosio A, Braud I, Chanzy A, Courault D, Demarty J, Kergoat L, Lewan E, Otlé C, Prévot L,  
22Zhao W, Calvet JC, Cayrol P, Jongschaap R, Moulin S, Noilhan J, Wigneron JP. 2002. SVAT  
23modelling over the Alpilles-ReseDA experiment: comparing SVAT models over wheat fields.  
24*Agronomie* **22**: 651-668.
- 25OTHU, 2010. <http://www.graie.org/othu/>. Consulted on 2010/01/06.

2

36

1

1Park SJ, van de Giesen N. 2004. Soil-landscape delineation to define spatial sampling  
2domains for hillslope hydrology. *Journal of Hydrology* **295(1-4)**: 28-46.

3Philip JR. 1969. Theory of infiltration. *Advances in Hydroscience* **5**: 215-296.

4R Development Core Team, 2004.R: a language and environment for statistical computing. R  
5foundation for statistical computing. Vienna, Austria. <http://www.r-project.org/>. Consulted on  
62010/01/06.

7Radojevic B. 2002. Méthode d'évaluation de l'influence urbaine sur le régime des crues d'un  
8bassin versant de 130 km<sup>2</sup>. Institut National des Sciences Appliquées de Lyon, Lyon.

9Randhir T. 2003. Watershed-scale effects of urbanization on sediment export: assesement  
10and policy, *Water Resources Research* **39(6)**, 1-13.

11Rawls WJ, Brakensiek DL. 1985. Prediction of soil water properties for hydrologic  
12modelling. In: *E.B.a.W.* Jones TJ (eds), *Watershed Management in the eighties*. ASCE,  
13Denver, April 30-May 1: 293-299.

14Reynolds WD, Bowman BT, Brunke RR, Drury CF, Tan CS. 2000. Comparison of tension  
15infiltrometer, and soil core estimates of saturated hydraulic conductivity. *Soil Science Society  
16of America Journal* **64**:478-484.

17Rogowski AS. 1971. Watershed physics: model of soil moisture characteristic, *Water  
18Resources Research* **12**: 513-522.

19Scalenghe R, Ferraris S. 2009. The First Forty Years of a Technosol. *Pedosphere* **19(1)**: 40-  
2052.

21Schmitt L, Grosprêtre L, Breil P, Lafont M, Vivier A, Perrin JF, Namour P, Jezequel C,  
22Valette L, Valin K, Cordier R, Cottet M. 2008. Préconisations de gestion physique de petits  
23hydrosystèmes périurbains : l'exemple du bassin de l'Yzeron (France). In. Actes du Colloque  
24« La gestion physique des cours d'eau : bilan d'une décennie d'ingénierie écologique »,

1

1 Verniers G, Petit F (eds), Namur, 10-12 oct. 2007, Groupe Interuniversitaire de Recherches en  
2 Ecologie Appliquée, Laboratoire d'Hydrographie et de Géomorphologie Fluviale, Direction  
3 des Cours d'Eau Non Navigables, Direction Générale des Ressources Naturelles et de  
4 l'Environnement - Ministère de Région wallonne : 177-186.

5 Schwarts R, Evett SR, Paul UW. 2003. Soil hydraulic properties of cropland compared with  
6 reestablished and native grassland. *Geoderma* **116**: 47-60.

7 SIRA, 2010. Sol Info Rhône-Alpes, [sira@rhone-alpes.chambagri.fr](mailto:sira@rhone-alpes.chambagri.fr) - [http://www.rhone-](http://www.rhone-8alpes.chambagri.fr/sira/)  
8 [alpes.chambagri.fr/sira/](http://www.rhone-alpes.chambagri.fr/sira/). Consulted on 2010/01/06.

9 Smettem KRJ, Parlange JY, Ross PJ, Haverkamp R. 1994. Three-dimensional analysis of  
10 infiltration from the disk infiltrometer. 1. A capillary-base theory, *Water Resources Research*  
11 **30**, 2925-2929.

12 Smiles DE, Knight JH. 1976. A note on the use of the Philip infiltration equation, *Australian*  
13 *Journal of Soil Science* **10**: 143-150.

14 Sobieraj JA, Elsenbeer H, Vertessy RA. 2001. Pedotransfer functions for estimating saturated  
15 hydraulic conductivity: implications for modelling stream flow generation. *Journal of*  
16 *Hydrology* **251**: 202-220.

17 SOeS, 2010. Service de l'Observation et des Statistiques, Occupation des Sols, Corine Land  
18 Cover, [http://www.ifen.fr/bases-de-donnees/occupation-des-sols-corine-land-cover.html?](http://www.ifen.fr/bases-de-donnees/occupation-des-sols-corine-land-cover.html?taille=)  
19 [taille=](http://www.ifen.fr/bases-de-donnees/occupation-des-sols-corine-land-cover.html?taille=). Consulted on 2010/01/06.

20 Stolte J, van Venrooij B, Zhang G, Trouwborst KO, Liu G, Ritsema CJ, Hessel R. 2003.  
21 Land-use induced spatial heterogeneity of soil hydraulic properties on the Loess Plateau in  
22 China. *Catena* **54**: 59-75.

23 van der Keur P, Iversen BV. 2006. Uncertainty in soil physical data at the basin scale - a  
24 review. *Hydrology and Earth System Sciences* **18**: 889-902

- 1van Genuchten MT. 1980. A closed-form equation for predicting the hydraulic conductivity  
2of unsaturated soils. *Soil Science Society of America Journal* **44** : 892-898.
- 3Vandervaere JP, Vauclin M, Elrick DE. 2000a. Transient flow from tension infiltrometers: I.  
4The two-parameter equation. *Soil Science Society of America Journal* **64**: 1263-1272.
- 5Vandervaere JP, Vauclin M, Elrick DE. 2000b. Transient flow from tension infiltrometers: II.  
6Four methods to determine sorptivity and conductivity. *Soil Science Society of America  
7Journal*, **64**: 1271-1284.
- 8Varado N, Braud I, Galle S, Le Lay M, Séguis L, Kamagate B, Depraetere C. 2006. Multi-  
9criteria assessment of the Representative Elementary Watershed approach on the Donga  
10catchment (Benin) using a downward approach of model complexity. *Hydrology and Earth  
11System Sciences* **10**: 427-442.
- 12Verecken H, Maes J, Darius P, Feyen J. 1989. Estimating the soil moisture retention  
13characteristics from texture, bulk density and carbon content. *Soil Science* **148**: 389-404.
- 14Wösten JHM. 1997. Pedotransfer functions to evaluate soil quality; In *Development in soils  
15sciences*, Gregorich E, Carter MR (eds)., Elsevier: Amsterdam; 221-245.
- 16Wösten JHM, Lilly A, Nemes A, Le Bas C. 1999. Development and use of a database of  
17hydraulic properties of European soils. *Geoderma* **90**: 169-185.
- 18Wösten JHM, Pachepsky YA, Rawls WJ. 2001. Pedotransfer functions: bridging the gap  
19between available basic soil data and missing soil hydraulic characteristics. *Journal of  
20Hydrology* **251**: 123-150.
- 21Xu X, Kiely G, Lewis C. 2009. Estimation and analysis of soil hydraulic properties through  
22infiltration experiments: comparison of BEST and DL fitting methods. *Soil Use and  
23Management* **25**: 354-361.
- 24Yilmaz D, Lassabatère L, Angulo Jaramillo R, Legret M. 2010. Hydrodynamic  
25characterization of BOF slags through adapted BEST method. *Vadoze Zone Journal* **9**: 1-10.



1

1Zhou X, Lin HS, White HS. 2008. Surface soil hydraulic properties in four soil series un  
2different land uses and their temporal changes. *Catena* **73**: 180-188.

1

1

## List of Figures

2

3Figure 1: Location of the Yzeron catchment and of the two experimental sub-catchments  
4(Mercier and Chaudanne). The grey scale shows the catchment slope with the highest values  
5in dark and the lowest values in white. The symbols indicate the location of rainfall (points)  
6and streamflow gauges (triangles).

7Figure 2: Pedology map of the Mercier catchment (from Sol Info Rhône Alpes, SIRA, 2010).  
8The various colors correspond to the various Soil Cartographic Units defined in Table I. The  
9symbols show the location of the infiltration test sites, with the various symbols  
10corresponding to the various land use defined in Table I.

11Figure 3: (a) Box plot of the fine particle size fractions and organic matter content (b) Box  
12plot of the dry bulk density and porosity of the topsoil. On the box plots, boundaries indicates  
13median, 25<sup>th</sup> and 75<sup>th</sup> quantiles, the top and bottom whiskers indicate the 10<sup>th</sup> and 90<sup>th</sup>  
14percentiles and the points the minimum and maximum values.

15Figure 4: Presentation of the sampled points in the USDA textural triangle. The various  
16symbols correspond to the different soil pedological units as defined in Table I.

17Figure 5: (a) Comparison of dry bulk density as measured using a 0-2.5 cm and 0-5 cm height  
18cylinder. (b) Relationship between dry bulk density and organic matter content.

19Figure 6. Observed (points) and fitted cumulative infiltration data for sites 41.1 (clearing) and  
2031-3 (orchards). The full line is the fit of Eq. (6) for short time steps and the dashed line is the  
21fit of Eq. (10) for large time steps. Eq. (6) was fitted to the points plotted with squares.

22Figure 7. Box plots of saturated hydraulic conductivity (single ring) and hydraulic  
23conductivity at -20 mm (mini-disk) for all the samples and the three identified classes KS1,  
24KS2 and KS3.

1

1Figure 8. Estimated retention curves and hydraulic conductivity curves for the combination of  
2classes DB1, DB2, DB3. Between near-saturated and saturated hydraulic conductivity, a  
3linear relationship on the natural logarithm of hydraulic conductivity versus soil water content  
4was assumed. The symbols are the saturated hydraulic conductivities for the various  
5combinations of DB and KS classes: broad leaved forest (DB1-KS1); coniferous forest (DB1-  
6KS3); permanent pasture (DB2-KS3); clearing (DB2-KS2); small woods (DB2-KS1);  
7cultivated pasture (DB3-KS2); crops (DB3-KS3)..

8Figure 9. Mapping of soil hydraulic properties. The classes numbering is provided in Table  
9VII. White surfaces correspond to the non sampled areas defined in Table VII.

10

11

12

13

14

1

1Table I. Number of sampled points for Single Ring (SR) and Mini-Disk (MDI) infiltration  
 2tests per Soil Cartographic Unit (SCU) and land use (figures in parentheses are the percentage  
 3of the total number of points). In the land use classes, we distinguish between “permanent  
 4pasture” (in place for more than 5 years) and “cultivated pasture” (in place for only one or a  
 5few years).

SCU number or land use	Number of SR tests	Number of MDI
<b>102</b> Loamy sand and clayey sand from gneiss and micaschist	15 (26%)	10 (23%)
<b>1031</b> Loamy sands from tuf within a forest dominated by coniferous	6 (10%)	7 (16%)
<b>7021</b> Loamy sands and clayey sands from colluvionated gneiss	15 (26%)	11 (25%)
<b>704</b> Colluvions loamy sand to clayey sand with slope	6 (10%)	4 (9%)
<b>7041</b> Colluvions loamy sand to clayey sand within talwegs	9 (16%)	5 (12%)
<b>7042</b> Alluvions clayey-sands to sandy clays within talwegs and narrow valleys	7 (12%)	6 (14%)
<b>Total</b>	<b>58</b>	<b>43</b>
<b>1</b> Permanent pasture	21 (36%)	14 (32%)
<b>2</b> Cultivated pasture	9 (15%)	7 (16%)
<b>3</b> Crop (wheat stubble)	3 (5%)	2 (5%)
<b>4</b> Crop (bare soil after ploughing)	4 (7%)	3 (7%)
<b>5</b> Orchards (peach, apples)	3 (5%)	2 (5%)
<b>6</b> Broad-leaved forest (oaks, chestnuts)	6 (10%)	6 (14%)
<b>7</b> Clearing	4 (7%)	2 (5%)
<b>8</b> Coniferous forest	4 (7%)	4 (9%)
<b>9</b> Small wood sometimes with ivy	4 (7%)	3 (7%)
<b>Total</b>	<b>58</b>	<b>43</b>

6

1

1Table II. Statistics of particle size data analysis, organic matter and shape parameters of the  
 2retention and hydraulic conductivity curves,  $n$  and  $\eta$ . CV is the coefficient of variation. The  
 3sample size is 28. Std stands for standard deviation

	Clay content	Fine silt content	Coarse silt content	Fine sand content	Coarse sand content	Organic matter content	$n$	$\eta$
Unit	%	%	%	%	%	g kg <sup>-1</sup>	-	-
Average	12.9	11.7	8.2	17.9	49.6	56.5	2.17	15.2
Std	4.0	3.5	2.5	3.6	10.4	26.9	0.045	3.2
Minimum	5.6	4.8	3.7	10.6	30.2	18.2	2.10	10.7
Maximum	22.7	20.1	13.7	23.8	73.4	133.0	2.26	22.8
CV (%)	13.8	29.9	30.5	20.1	21.0	47.6	2.1	21.0

4

5

1

1Table III. Average and standard deviation (std in parentheses) organic matter content, dry bulk density, porosity, sorptivity and hydraulic  
 2conductivity derived from the single ring (SR) infiltration tests in terms of land use class.

Land use	Sample size	Organic matter content	Sample size dry bulk density and SR	Dry bulk density	Porosity	Sorptivity SR	Saturated hydraulic conductivity SR
Units	-	g kg <sup>-1</sup>	-	kg m <sup>-3</sup>	-	mm s <sup>-1/2</sup>	mm s <sup>-1</sup>
Permanent pasture	11	61.3 (10.9)	21	969 (122)	0.63 (0.05)	3.15 (2.45)	0.51 (0.75)
Cultivated pasture	4	35.6 (12.9)	9	1269 (305)	0.52 (0.11)	1.64 (0.58)	0.11 (0.08)
Crops (wheat stubble)	1	19.5 (NA)	3	1411 (24)	0.47 (0.01)	2.8 (0.76)	0.28 (0.10)
Crops (bare soil after ploughing)	1	18.2 (NA)	4	1549 (265)	0.41 (0.10)	0.84 (0.83)	0.13 (0.21)
Orchards (peach, apple)	1	28.3 (NA)	3	1472 (225)	0.44 (0.08)	3.62 (2.10)	0.40 (0.27)
Broad-leaved forest	3	88.8 (54.1)	6	676 (146)	0.74 (0.05)	4.86 (1.45)	1.32 (0.57)
Clearing	3	51 (21.2)	4	1180 (283)	0.55 (0.11)	1.16 (0.40)	0.05 (0.02)
Coniferous forest	1	84.5 (NA)	4	725 (130)	0.73 (0.05)	1.50 (0.91)	0.23 (0.15)
Small wood sometimes with ivy	3	65 (19.3)	4	1058 (292)	0.60 (0.11)	5.77 (2.12)	1.50 (0.62)
All	28	56.5 (26.6)	58	1078 (318)	0.59 (0.12)	2.87 (2.18)	0.50 (0.67)

3

1

1Table IV. Statistics of organic matter content, dry bulk density, porosity and ratio (final water content/porosity) for the three main land use  
 2classes where significant differences were identified: class DB1: broad leaved forest + coniferous forest, class DB2: permanent pasture + clearing  
 3+ small woods, class DB3: cultivated pasture + crop (wheat stubble) + crop (bare soil after ploughing) + orchards. Std stands for standard  
 4deviation

	Units	Number of samples	Organic matter	Dry bulk density	Porosity	Ratio final water content / porosity
		(-)	(g kg <sup>-1</sup> )	(kg m <sup>-3</sup> )	(-)	(-)
Class DB1	Average	10	103.0	695	0.74	0.66
	(Std)		(24.4)	(135)	(0.05)	(0.16)
	[Min-Max]	-	[62.6-133]	[472-817]	[0.69-0.82]	[0.32-0.81]
Class DB2	Average	29	60.5	1010	0.62	0.69
	(Std)		(13.6)	(185)	(0.07)	(0.17)
	[Min-Max]	-	[26.5-86.3]	[685-1424]	[0.46-0.74]	[0.30-1.0]
Class DB3	Average	19	30.7	1382	0.48	0.70
	(Std)		(12.3)	(270)	(0.10)	(0.18)
	[Min-Max]	-	[18.2-53.3]	[846-1852]	[0.30-0.68]	[0.35-1.0]

5

6

1

1Table V. Statistics of maximum infiltrated depth,  $I_{max}$ , maximum infiltration time,  $t_{max}$ , and  
 2their ratio,  $L$ , for the single ring infiltration tests

Variable	Average (-)	Standard deviation (-)	Minimum (-)	Maximum (-)	Median (-)	Coefficient of variation (-)	Sample size
$I_{max}$ (mm)	86.6	18.1	11.5	114.4	90	0.21	58
$t_{max}$ (min)	10.3	19.3	0.25	114.4	2.95	1.87	58
$L$ (mm min <sup>-1</sup> )	55.9	79.6	0.36	340	26.7	1.42	58



1

1Table VI. Statistics of sorptivity  $S$ ,  $S$ , saturated hydraulic conductivity, sorptivity MDI, hydraulic conductivity at -20mm for the three main land  
 2use classes where significant differences were identified: class KS1: broad leaved forest + small woods, class KS2: cultivated pasture + crop  
 3(bare soil after ploughing) + clearing, class KS3: permanent pasture + crop (wheat stubble) + coniferous forest + orchard. Std stands for standard  
 4deviation.

5

		Number of samples SR	$S$ ( $\text{mm s}^{-1/2}$ )	$K_s$ ( $\text{mm s}^{-1}$ )	$h_{VG}$ (mm)	Number of samples MDI	$S(h=-20\text{mm})$ ( $\text{mm s}^{-1/2}$ )	$K_s(h=-20\text{mm})$ ( $\text{mm s}^{-1}$ )	$K_s/K_s(h=-20\text{mm})$ (-)
	Units	(-)	( $\text{mm s}^{-1/2}$ )	( $\text{mm s}^{-1}$ )	(mm)	(-)	( $\text{mm s}^{-1/2}$ )	( $\text{mm s}^{-1}$ )	(-)
Class KS1	Average	10	5.22	1.39	-72.2	7	0.08	0.0031	448
	(Std)		(1.70)	(0.56)	(56.5)		(0.05)	(0.0027)	
	Median		4.64	1.20	-55.2		0.10	0.0021	571
	CV (%)		32.6	40.3	78.2		62.5	87.1	
Class KS2	Average	17	1.34	0.10	-74.0	12	0.11	0.0039	26
	(Std)		(0.67)	(0.11)	(60.3)		(0.05)	(0.0028)	
	Median		1.20	0.06	-65.5		0.10	0.0029	21
	CV (%)		50.0	110.0	81.5		45.4	71.8	
Class KS3	Average	30	2.95	0.44	-63.5	20	0.10	0.0075	59
	(Std)		(2.18)	(0.63)	(41.8)		(0.05)	(0.0067)	
	Median		2.47	0.24	-64.7		0.09	0.0049	49
	CV (%)		73.9	143.2	65.8		50.0	89.3	
All	Average	57	0.59	2.87	-68.1	37	0.10	0.0056	515
	(Std)		(0.12)	(2.18)	(49.8)		(0.052)	(0.0054)	
	Median		2.05	0.22	-64.8		0.10	0.0047	47
	CV (%)		20.3	76.0	73.1		52.0	96.7	

6

2

48

1

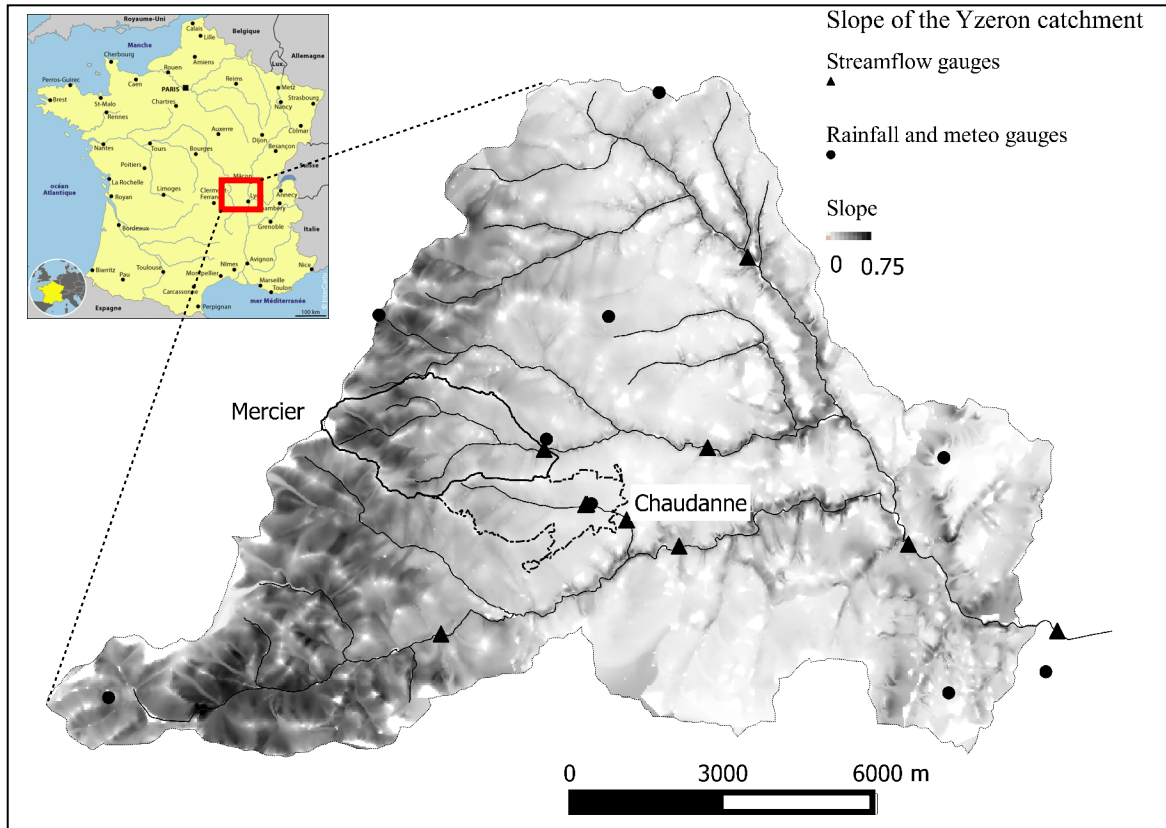
1Table VII. Correspondence between the original detailed land use map of the Mercier catchment and the reclassified map according to the dry  
 2bulk (DB) and saturated hydraulic conductivity (KS) classes for mapping of porosity, saturated water content and saturated hydraulic  
 3conductivity.

Reclassified land use class	Original classes of the Mercier land use map	Porosity (-)	Saturated water content ( $\text{m}^3 \text{m}^{-3}$ )	Near saturated hydraulic conductivity (-20 mm pressure) ( $\text{mm s}^{-1}$ )	Saturated hydraulic conductivity ( $\text{mm s}^{-1}$ )
DB1-KS1 (11)	Broad-leaved forest,	0.74	0.49	0.0031	1.39
DB1-KS3 (13)	Coniferous forest	0.74	0.49	0.0075	0.44
DB2-KS1 (21)	Scattered trees, hedges,	0.62	0.43	0.0031	1.39
DB2-KS2 (22)	Moors, heathland, fallow land,	0.62	0.43		
DB2-KS3 (23)	Pasture	0.62	0.43	0.0075	0.44
DB3-KS2 (32)	Ploughed fields, scattered grass,	0.48	0.34		
DB3-KS3 (33)	Orchards, berry plantation, wasteland, dump sites, spaces under construction, cemeteries	0.48	0.34	0.0075	0.44
Not sampled during the campaign	Impermeable surface (cement, asphalt), road networks, dirt roads, pervious artificial surfaces (gardens, trees)	Literature	Literature	Literature	Literature
Not relevant	Water bodies	NA	NA	NA	NA

4

1

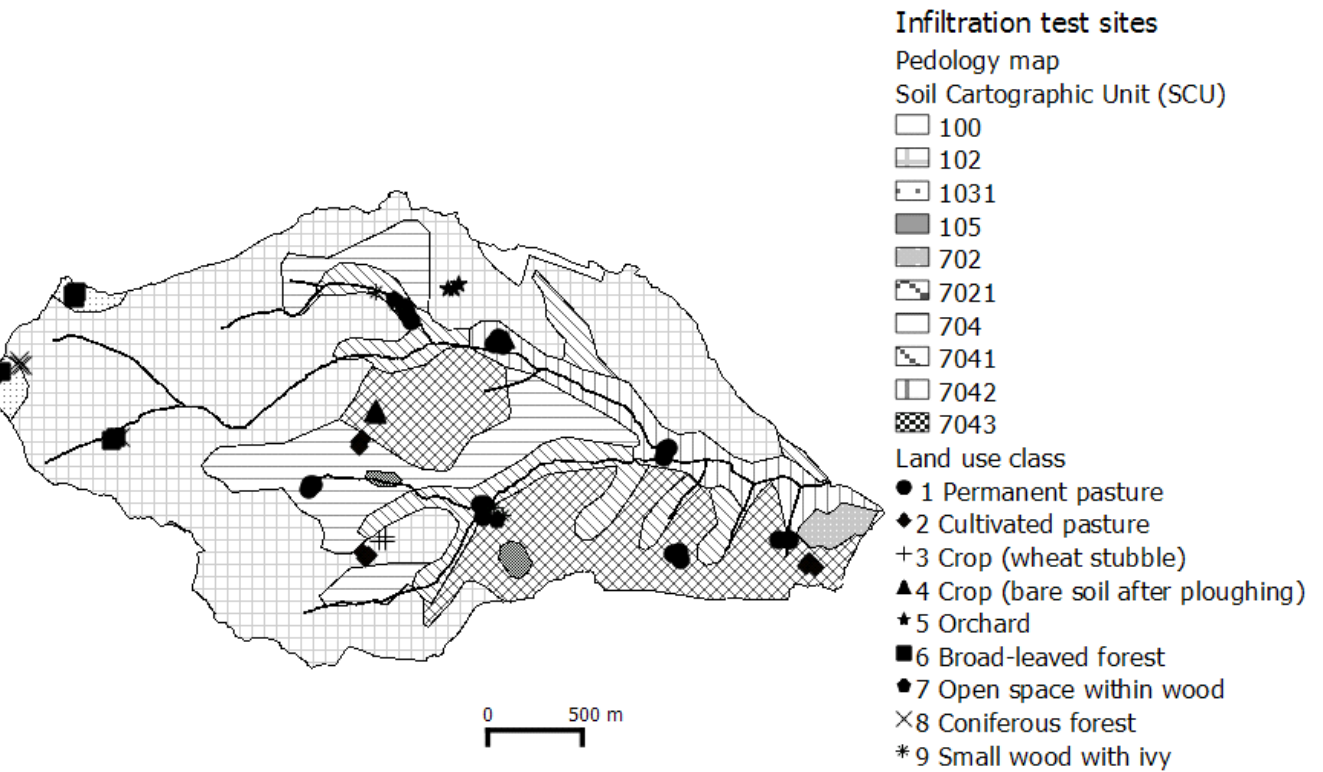
1



2

3Figure 1: Location of the Yzeron catchment and of the two experimental sub-catchments  
4(Mercier and Chaudanne). The grey scale shows the catchment slope with the highest values  
5in dark and the lowest values in white. The symbols indicate the location of rainfall (points)  
6and streamflow gauges (triangles).

1  
1  
2  
3  
4  
5  
6  
7  
8  
9  
10  
11  
12  
13  
14  
15  
16  
17

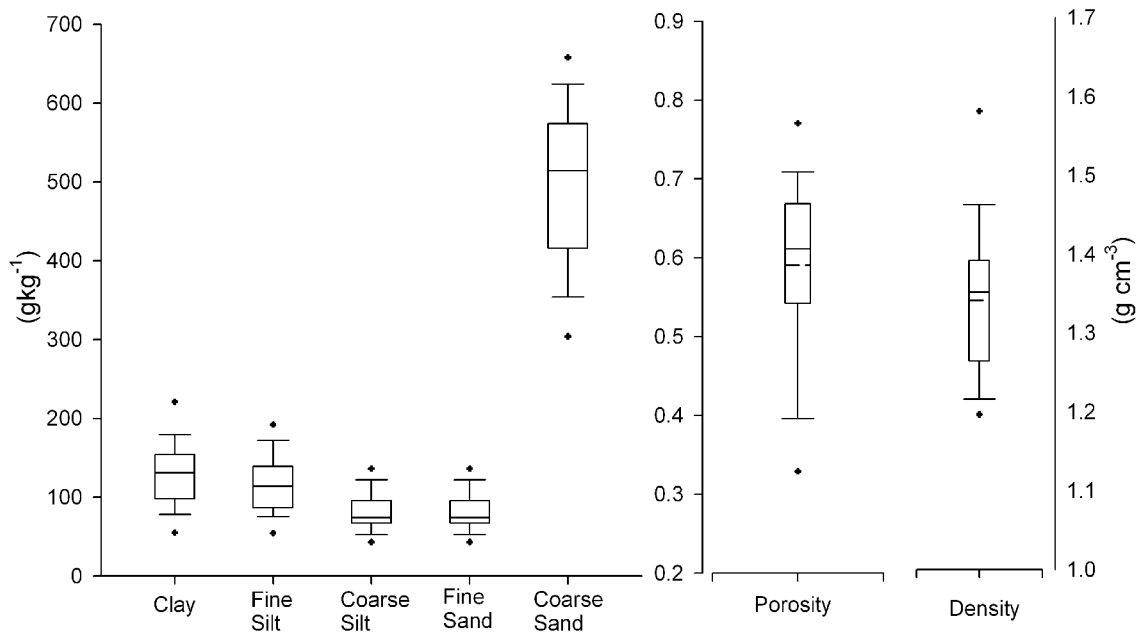


18Figure 2: Pedology map of the Mercier catchment (from Sol Info Rhône Alpes  
19<http://www.rhone-alpes.chambagri.fr/sira/> ). The various colors correspond to the various Soil  
20Cartographic Units defined in Table I. The symbols show the location of the infiltration test  
21sites, with the various symbols corresponding to the various land use defined in Table I

22  
23  
24  
25

1

1

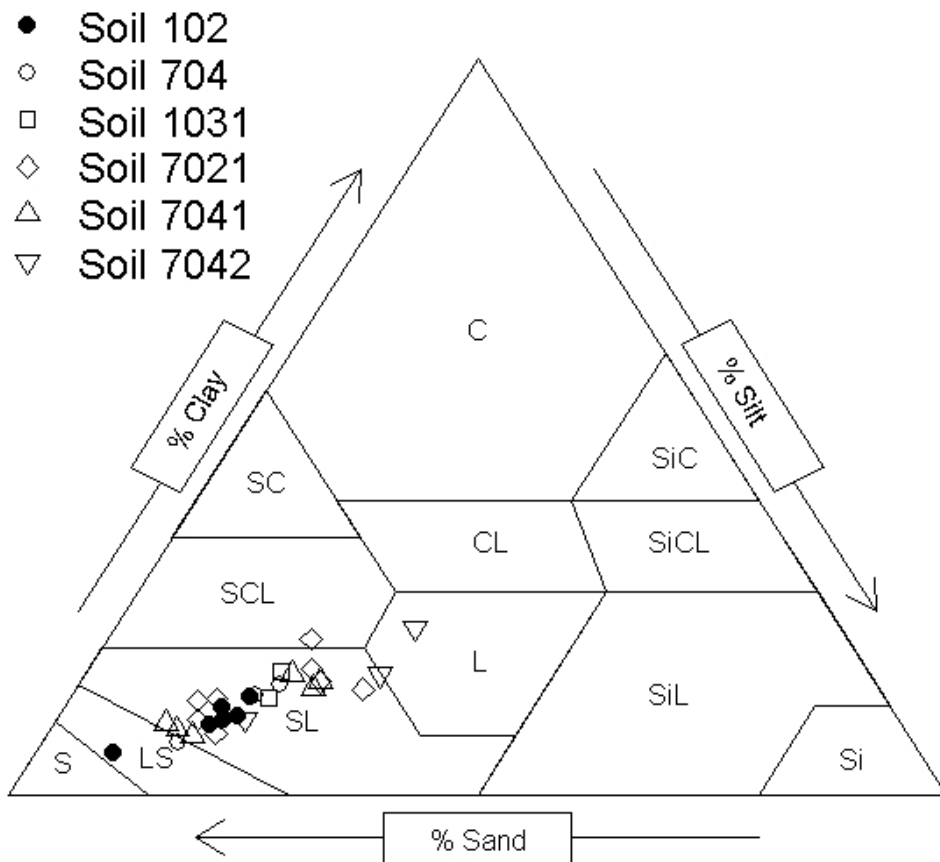


2

3Figure 3: (a) Box plot of the fine particle size fractions and organic matter content (b) Box  
4plot of the dry bulk density and porosity of the topsoil. On the box plots, boundaries indicates  
5median, 25<sup>th</sup> and 75<sup>th</sup> quantiles, as vertical boxes error bars respectively: the top and bottom  
6whiskers indicate the 10<sup>th</sup> and 90<sup>th</sup> percentiles and the points the minimum and maximum  
7values.

2

1

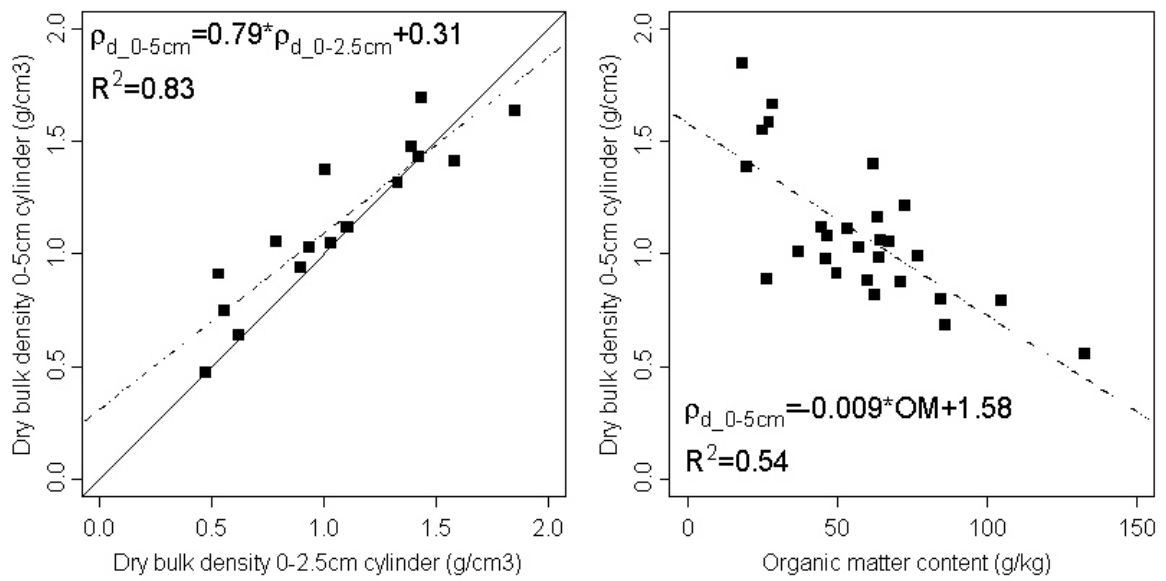


1

2

3 Figure 4: Presentation of the sampled points in the USDA textural triangle. The various  
4 symbols correspond to the different soil pedological units as defined in Table I..

1



1

2Figure 5: (a) Comparison of dry bulk density as measured using a 0-2.5 cm and 0-5 cm height  
3cylinder. (b) Relationship between dry bulk density and organic matter content.

1

1

2

3

4

5

6

7

8

9

10

11

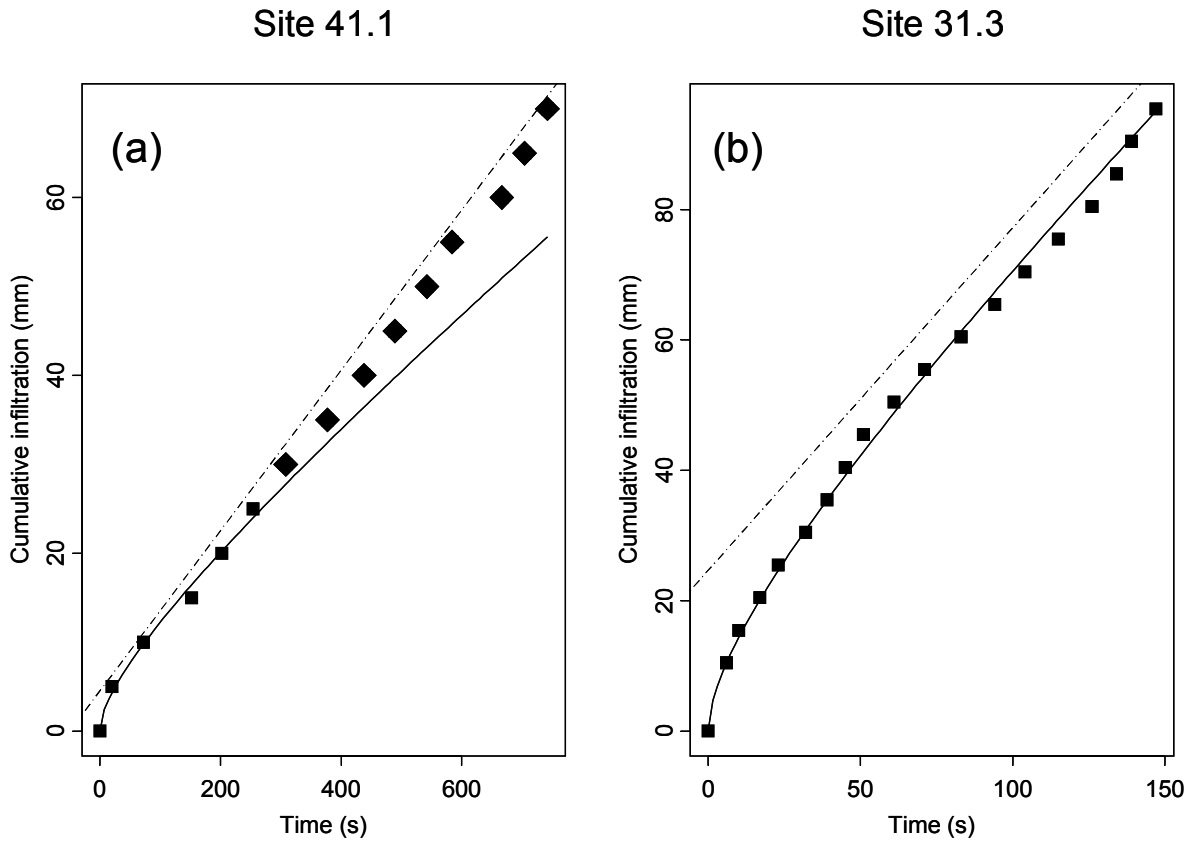
12

13

14

15

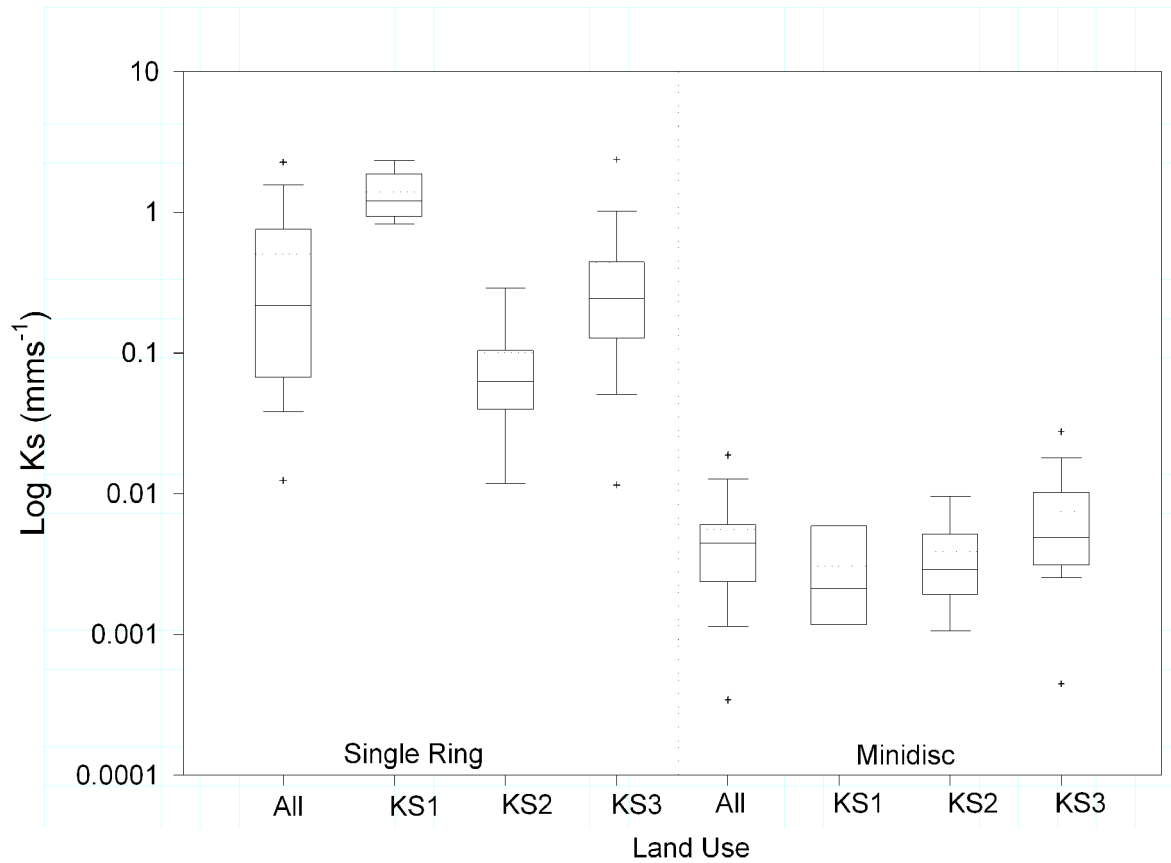
16



17Figure 6. Observed (points) and fitted cumulative infiltration data for sites 41.1 (Open space  
18in forest) and 31-3 (orchards). The full line is the fit of Eq. (6) for short time steps and the  
19dashed line is the fit of Eq. (10) for large time steps. Eq. (6) was fitted to the points plotted  
20with squares.



1

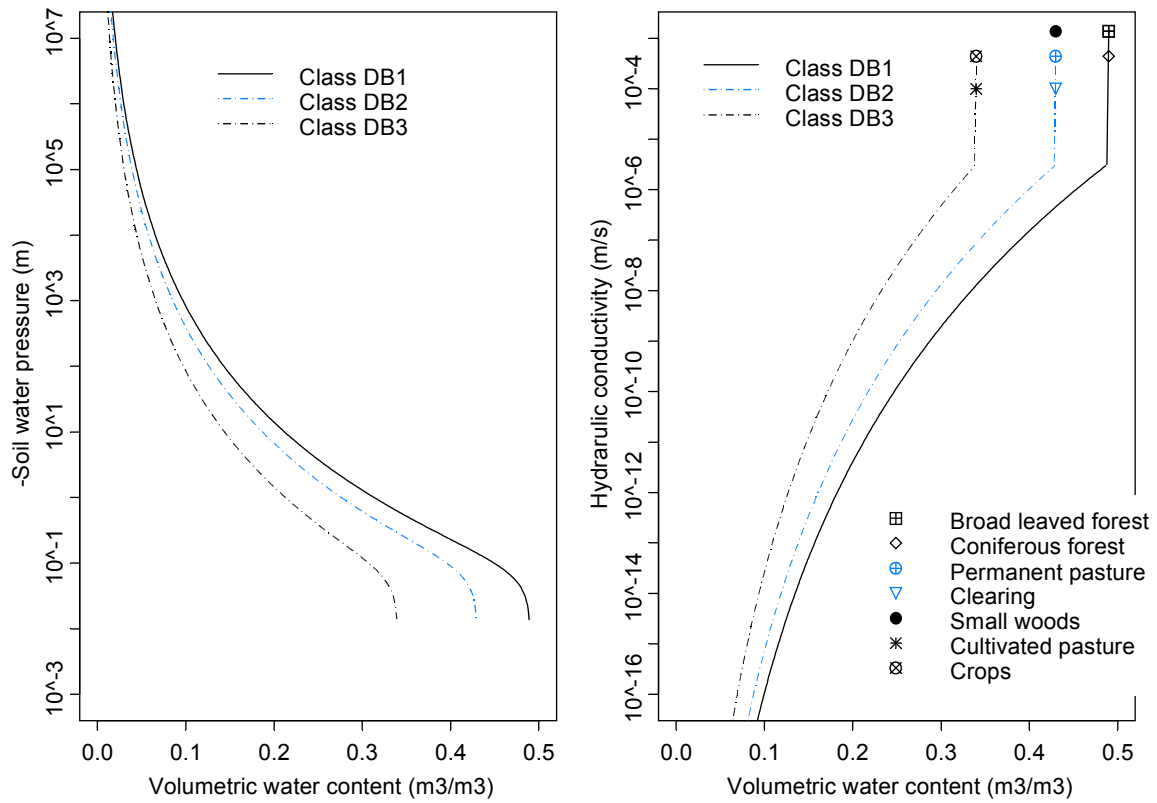


1

2 Figure 7. Box plots of saturated hydraulic conductivity (single ring) and hydraulic  
3 conductivity at -20 mm (mini-disk) for all the samples and the three identified classes  
4 KS1, KS2 and KS3.  
5

1

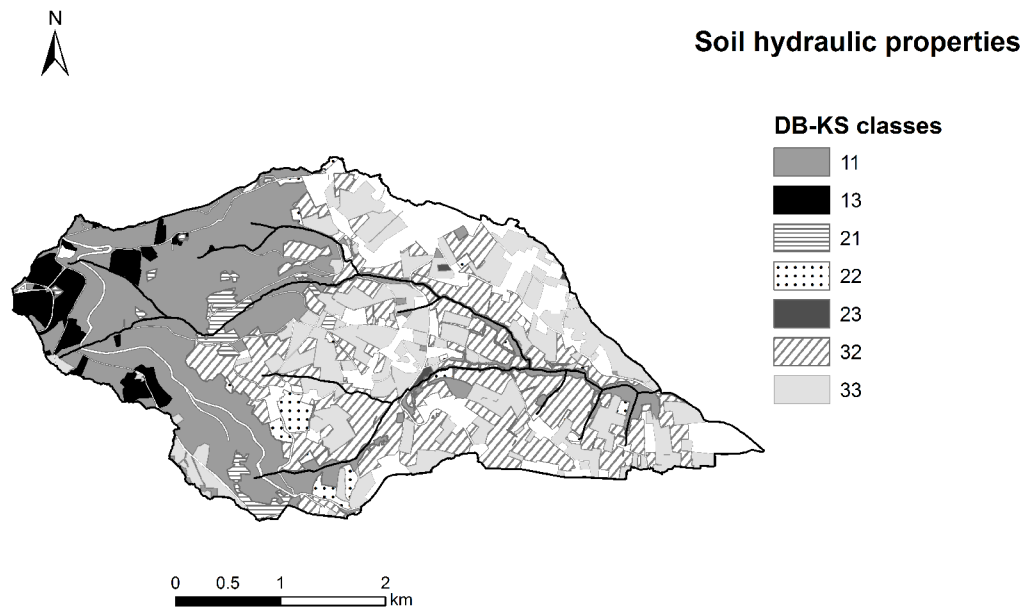
1



2

3Figure 8. Estimated retention curves and hydraulic conductivity curves for the combination of  
 4classes DB1, DB2, DB3. Between near-saturated and saturated hydraulic conductivity, a  
 5linear relationship on the natural logarithm of hydraulic conductivity versus soil water content  
 6was assumed. The symbols are the saturated hydraulic conductivities for the various  
 7combinations of DB and KS classes: broad leaved forest (DB1-KS1); coniferous forest (DB1-  
 8KS3); permanent pasture (DB2-KS3); clearing (DB2-KS2); small woods (DB2-KS1);  
 9cultivated pasture (DB3-KS2); crops (DB3-KS3)..

1



1

2Figure 9. Mapping of soil hydraulic properties. The classes numbering is provided in Table  
3VII. White surfaces correspond to the non sampled areas defined in Table VII.